NASA TECHNICAL MEMORANDUM NASA TM-88446

CYROGENIC WIND TUNNELS - PROBLEMS OF CONTINUOUS OPERATION AT LOW TEMPERATURES

D. Failmann

Translation of "Souffleries Cyrogeniques - Problemes lies au fonctionnement continu en basse temperature, O.N.E.R.A., Report No. OA n. 9/5007 AYD (DERAT no. 9/5007 DY), Centre d'Etudes et de Recherches de Toulouse, France, June, 1980, pp. 1-18 (plus figures).

NATIONAL AERONAUTICS AND SPACE ADMINISTRATION
WASHINGTON D.C. 20546 JUNE 1986

STANDARD TITLE PAGE

1. Report No.	2. Government Accession No.	3. Recipient's Catalog No.
NASA TM-88446		

4. Title and Subtitle	5. Report Date
CYROGENIC WIND TUNNELS - PROBLEMS OF CONTINUOUS OPERATION AT LOW TEMPERATURES	June 1986
	6. Performing Organization Code

7. Author(s)	8. Performing Organization Report No.
D. Faulmann	NASW-4005
	10. Work Unit No.

9. Performing Organization Name and Address	11. Contract or Grant No.
Leo Kanner Associates Redwood City, CA 94063	13. Type of Report and Period Covered Translation
12. Sponsoring Agency Name and Address National Aeronautics and Space Administration, Washington D.C. 20546	14. Sponsoring Agency Code

15. Supplementary Notes

Translation of "Souffleries Cyrogeniques - Problemses lies au fonctionnement continue en basse temperature, O.N.E.R.A. Report No. OA n. 9/5007 AYD (DERAT n. 9/5007 DY), Centre d'Etudes et de Recherches de Toulouse, France, June, 1980, pp. 1-18 (plus figures).

16. Abstract

This report describes the design of a cyrogenic wind tunnel operating continuously, capable of attaining transonic speeds at generating pressures of about 3 bars. Its stainless steel construction with inside insulation allows for very rapid temperature variations promoted by rapid changes in the liquid nitrogen flow.

A comparative study of temperature measuring probes shows a good reliability of "thin sheet" thermocouples. To measure fluctuations, only a "cold wire" makes it possible to record frequencies of about 300 Hz.

The use of an integral computer method makes it possible to determine the impact of the wall temperature ratio to the adiabatic wall temperature for the various parameters characterizing the boundary layer. These cases are processed with positive and negative pressure gradients.

17. Key Words (Selected by Author(s))	18. Distribution Statement
Cyrogenic wind tunnels - Induction wind tunnels - Thermal turbulence - Aerodynamic noise - Liquid nitrogen injection	Unclassified-Unlimited

19. Security Classif. (of this report)	20. Security Classif. (of this page)	21. No. of Pages	22.
Uncalssified	Unclassified		

SUMMARY

Description of the adjustment of a cyrogenic wind tunnel under continuous operation, capable of attaining transonic speeds at generating pressures of about 3 bars. Its construction in stainless steel with an inside insulation permits very rapid temperature variations caused by rapid changes in the liquid nitrogen flow.

A comparative study of probes for measuring temperatures shows a good reliability of "thin sheet" thermocouples. To measure fluctuations, only a "cold wire" makes it possible to record frequencies of about 300 Hz.

The use of an integral computer method makes it possible to determine the impact of the wall temperature ratio to the adiabatic wall temperature for the various parameters characterizing the boundary layer. These cases are processed with positive and negative pressure gradients.

TABLE OF CONTENTS

CYROGENIC WIND TUNNELS - PROBLEMS OF CONTINUOUS OPERATION AT LOW TEMPERATURES

D. Faulmann

1 - STUDY OBJECTIVE

To conduct a study on a small available installation of the essential problems which arise for the operation of wind tunnels at low temperatures both from the standpoint of performance and flow qualities, and from the standpoint of instrumentation and measuring instruments.

To specifically analyse the impact of a wall temperature which may be different from the adiabatic on the boundary layer characteristics.

The activities developed were divided into three phases:

.Phase 1: Development and implementation of a small pilot installation operating continuously: cyrogenic T'3 wind tunnel.

.Phase 2: Experimental technique and instrumentation for measurementes in a cyrogenic environment.

.Phase 3: Problems associated with thermal flows and with wall temperatures.

2 - BENEFIT OF THE STUDY

2.1 - Specific Research Objectives

To use a pilot installation under continuous operation to study the problems and to define the solutions relevant to cyrogenic wind tunnels under continuous operation. To very specially analyze the qualities of the flow as a function of the various

factors which the various consecutive elements represent.

.To design and implement in the available installation various experimental systems permitting the completest possible characterization of the flow magnitudes at low temperatures.

.To fundamentally study the impact of an essential similarity parameter which is the ratio of the wall temperature to the adiabatic wall temperature on the boundary layer characteristics.

2.2 Background of the Study and Previous Results Obtained

Construction of a typical circuit of a cyrogenic wind tunnel operating continuously permitting flows at temperatures in the vicinity of 120°K and pressurable to 3 bars. It was turned on in the /3
first phase with a low power blower, creating a flow at a temperature of about 120°K for low speeds.

Methods were established at DERAT for calculating turbulent boundary layers for compressible flows to be used to study the impact of the wall temperature.

3 - CONDUCTING THE STUDY

3.1 - Summary of the Various Phases

Phase 1

T'3 wind tunnel equipment of a blower with a large compression ratio and driven by a variable speed engine with a power of 125 KW. The performance was tested. The test section was adapted to allow transonic speeds to be reached.

The operation of the cyrogenic wind tunnel was adjusted: flows were created for various temperature levels and for various Mach numbers in the test section.

Initial flow quality studies: measurement of the spatial gradients and the temperature fluctuations.

Phase 2

To compare and test different measuring techniques to qualify flows at low temperatures. To develop experimental techniques for cyrogenic installations. Knowledge of the various flow parameters at low temperatures is indispensable for cases of steady flows. It becomes fundamental for cases of unsteady phenomena which occur, for example, when starting up of gust wind tunnel or when the test conditions are rapidly changed in a wind tunnel under continuous operation.

Phase 3

Development of an integral computer method to determine the impact of the wall temperature on the characteristics of turbulent boundary layers: case of a negative pressure gradient and finally, case of a positive pressure gradient which may lead to separation.

3.2 - Results Obtained

3.21 Tests on a Continuous T'3 Cyrogenic Pilot Installation

Figures 1 and 2 shows the T'3 continuous cyrogenic wind tunnel which is made up of the following elements:

1) - Test section: 100 x 120 mm^2 section. The two side gates /4 installed on hinges, each of which has three windows, two of which have a 50 mm diameter, and one a 150 mm diameter.

As shown in figure 3, the slope of the upper and lower wall may be adjusted using screw jacks. Each wall is equipped with 10

static taps.

2) The neck element is equipped with two screw jacks permitting a connection to the walls of the test section on the one hand and, the formation of a neck in the case of a transonic operation. The outlet section remains stationary (100 x 160 mm^2). Five upper and lower static taps are connected with those of the test section to a scanivalve connector attached to one of the three doors of the box of the test section. Test section length: 600 mm, neck element: 300 mm.

3) Rectangle-circle transformation piece: length 500 mm, inlet section 100 x 160 mm^2, outlet diameter DN 150.

4) Nozzle: inlet diameter DN 150, outlet diameter DN 250, length 1,000 mm.

5) Elbow no. 1 DN 250. Spacing 300 mm. It has 5 blades made up of a 3 mm thick sheet, bent by a 800 radius followed at the trailing edge by a straight part 30 mm long. This straight part is inclined about 5° to the inside with respect to the bend axis. The blades are soldered on the inside by an ellipsis 140 mm high and 10 mm thick.

6) DN 250 van end, height 200 mm. It is equipped with four DN 50 tappings placed at 90°. They may be used for observation or for injecting liquid nitrogen.

7) Elbow no. 2 DN 250. Same design as elbow no. 1, but its attachment is over the overmultiplier and the sleeve of a transmission shaft made up of a tube which maintains the atmospheric pressure in the casing and in the compressor bearing system.

8) Compressor element.

9) Return circuit: DN 250 inlet diameter, DN 350 outlet diameter, length 1,200 mm. Four tappings with a DN 50 diameter equip this element.

10) Cone, length 900 mm, with DN 350 - DN 400 diameters.

11) DN 400 cylindrical element, length 700 mm, also equipped with four DN 50 tappings. It also has the support of the wind tunnel and allows the wind tunnel to expand longitudinally, with the fixed point being the geared motor located near bend no. 2.

12) Bend no. 3. Same manufacture as bend no. 1 and 2. /5

13) Bend no. 4. Identical to preceding bend.

14) Plenum chamber. A cone followed by a cylindrical part constitutes the carcass of this part which holds the pressure. In contrast the covering is made of a thin 1.5 mm stainless steel sheet and has a 400 mm x 400 mm, 290 mm long square-circle transformation element, three 400 x 400 mm frames 100 mm long and a convergent 290 mm long. At the outlet of the transformation element there is an aluminum honeycomb 40 mm long, with a 6 mm mesh. Two grids are clamped between 400 x 400 mm frames. A cloth filter 10 mm thick (P 15 500 cadi) is attached in front of the last grid. Any fittings with the convergent is attached on one side to a DN 600 flange provided with a 100 x 120 mm opening (with the insulator). The other side of this flange receives the test section.

Thermal insulation applied to the inside of the continuous wind tunnel has the great advantage of being able to vary the temperature in relatively short periods of time, because it is not necessary to cool the outside casing too which undergoes pressure stresses. This condition of a large dT/dt gradient obviously requires a low heat storage capacity on the surface. In the case

of use in T'3, we are satisfied with a 5 mm thickness, since this dimension was suitable for insulating the T2 gust wind tunnel with an operating time of about 30 seconds.

The use of two insulators and four different glues allowed us to test several combinations in the various sections of the circuit.

The insulators used were the following:

a - Cork agglomerated with Triplex, 5 mm thickness;
b - Rigid polyurethane foam (Klegecell) with Triplex, 5 mm thickness.

"Triplex" is made up of an aluminum sheet, with a thickness of e = 40 μ, glued between two fiberglass fabric sheets and coated with a polyurethane based glue. The advantege of this layer glued to the insulator consists of making the insulator impervious and protecting it from possible abrasion. The disadvantage, on the other hand, lies in the greater surface heat storage capacity, resulting in a greater liquid nitrogen consumption and in the potential for establishing a heat gradient as a function of a shorter time.

Five glues were tested:

a - Sapropene or Bostik; contact glue.
b - Elastuff 504 (DOW): polyurethane based glue, 1/1 mixture, /6 fast drying.
c - Macroplast UK 8202/UK 5430 (HENKEL). Polyurethane based adhesive free of solvents, 1/4 mixture, easy to use

d - Resin XF 415 A/XF 415 B (PROCHAL). Epoxy resin based adhesive containing no solvent, 3/1 mixture, highly viscous paste.

e - Araldite AV 144/HV 997 (CIBA-GEIGY). Epoxy resin adhesive without solvent, 3/2 mixture, highly viscous paste.

The following combinations are shown in figure 1:

1 and 2: side walls: Klegecell + Macroplast 8202
top wall: Cork + Elastuff 504
bottom wall: Kegecell + Elastuff 504
3: Cork + Prochal 415
4: Cork + Prochal 415
5: Cork + Macroplast 8202
6: Cork + Macroplast 8202
7: Cork + Prochal 415
9: Kegecell + Macroplast 8202
10: Klegecell + Elastuff 504
11: Klegecell + Elastuff 504
12: Klegecell + Macroplast 8202
13: Klegecell + Macroplast 8202
14: Klegecell + Macroplast 8202
15: Transformation piece: Cork + Saproprene
Frames: Cork + Saproprene
Convergent: Cork + Araldite

For the bends, the parts between the blades were covered with cork and fastened with Saproprene or Bostik type contact glue.

The blades themselves are not heat insulated.

Given the dimensions of the wind tunnel and the electrical availability, we limited the power of the driving system to 125 KW.

Figure 4 shows a sectional view of the axial compressor, the connector of the driving pin in its sleeve, the 3,000 - 11,4000 rpm multiplier with a gear stage and the speed changeable engine.

The multiplier and the engine are mounted over a chassis

which holds at the same time bend no. 2 and therefore the entire rear part of the wind tunnel. A Rilson pad placed under the support of part no. 11 allows the system to expand.

The one-stage compressor (Technofan ECT 900-118) is made up of a 14-blade wheel with one 57° bitangent. A nozzle equipped with 17 blades (79.55° bitangent) is placed downstream from the wheel. The system is fastened with three arms in the entirely stainless steel cylindrical carcass and which has no inside insulation.

A rib is placed upstream and downstream from the compressor. The wheel and rectifier are made of AS 7 G 06 and are subjected to a Y 23 heat treatment. The annular passage section is formed by the outside diameter of 247 mm and the hub diameter of 190 mm.

The wheel is driven by the transmission shaft (which can revolve 11,400 rpm) which crosses bend no. 2 in a 40 mm diameter sleeve. Seals placed after the compressor bearings make it possible to maintain the atmospheric pressure in the casing as well as in the sleeve.

The oil tank is placed under the multiplier. The multiplier and wheel bearing lubricator uses high fluidity oil, even at temperatures as low as -50°C (Aeroshell Fluide 4). A pressure controller monitors the lubrication pressure. In contrast, a thermostat placed on the oil return circuit of the compressor actuates a heating resistance in the oil tank when the oil temperature drops too low.

The multiplier with a 3.8 ratio is driven by a C.E.M. d.c. engine with a power of 125 KW. The regulated rotation speed is displayed using a thyristor variator and may vary between 0 and 3,000 rpm. By subsequently connecting it to a computer it is possible to vary the rotation speed very rapidly and to thus create

Mach number levels which should be accompanied by an increase or decrease in the nitrogen rate if the temperature is to be kept constant.

Figure 5 shows the theoretical compressor characteristics. Figure 6 show the results obtainedwhen the equipment is accepted and transposed for cyrogenic conditions. These tests were conducted with suction in the open air. Figure 7 gives a comparison of the Δp value measured at the time of acceptance in the T'3 wind tunnel.

Compared to the preceding system, for the case of very low speeds, the liquid nitrogen injection system was modified only very slightly. Rather than injecting in the direction of the flow, we mounted the nozzles so that they be tangential to the wall and sprayed perpendicular to the flow. Four nozzles may therefore be /8 installed in the three tapping sections: NW 50(6), (9) and (11).

Figure 8 shows one of the nozzles on an NW 50 flange.

To increase the evaporation distance as far as possible in the aerydynamic circuit and to benefit from a high kinetic energy, we finally mounted the four nozzles at the outlet of the circle-square transformation piece (3) behind the test section. The rods bearing sprayers are secured by a Teflon disk and clamped between DN 150 flanges with fastener bolts.

In regard to storage and the liquid nitrogen injector (figure 9), we simply increased the tappings on the liquid outlet of the tank. The small dimension of the pipes (1/2") does not make it possible to have large liquid flows when operating at high Mach numbers and pressures of about 3 bars.

Figure 10 shows the capabilities for a rapid variation of the Mach number (at ambient temperature).

Plate 11 shows the Mach variation as a function of the temperature for p_i = 1 bar and 9,880 rpm.

Figures 12 and 13 show a standard test for the temperature and Mach number as a function of time.

3.22 - Experimental And Instrumentation Techniques

To qualify low temperature flows, we had to develop different measuring techniques and compare them. In particular we tested the means for measuring temperatures and their fluctuations. These values are not only high for a wind tunnel under continuous operation, but they are also necessary to characterize the process of rapid changes in the test conditions and for all unsteady phenomena occurring, for example, when a gust wind tunnel is put into service.

To measure the temperatures, we have:

Platinum resistors which are also used for calibrating other measuring systems. The response time of these probes is very high. A platinum wire wound around a silicon rod and covered with an insulator for protection (resistance of about 100 Ω) is used.

The thermocouples: For the temperature level which interests us, the use of constant copper wires is generally recommended. The wire diameter (about 1/10 mm) and the weld determines the response time (a few Hz). The aging of the weld (preferably electrical) alters the measuring reliability of the couples.

A very definite improvement in the measuring accuracy via electromotive force is provided by sheet thermocouples made by an evaporation process under vacuum. The thickness is so thin that the thermocouple must be maintained over a think insulating sheet. The response time is definitely higher compared to conventional thermocouples.

To measure the temperature fluctuations, we tested cold wires which are therefore heat-resistant sensors powered under a low current (hot wire). The sensors used, during tests performed by DERMES are made from standard supports (55-P-01 type DISA probes) equipped with platinized tungsten wires with a 9 μ diameter. This diameter was adopted for reasons of mechanical strength. Preliminary tests showed an excessive fragility of wires with smaller diameters (2.5 or 5 μ), for flow velocities exceeding M = 0.2.

The sensors were calibrated between 300°K and 110°K and the results showed a linear response and sensitivity of 5 mV/K for the measuring current used. The measuring equipment is made up of a constant current power supply (I = 4 mA), the voltage received at the terminals of the sensor is then amplified in a 100 ratio. For such power conditions and in flows with velocities exceeding M = 0.2, the self-heating of the wire due to the power dissipated by Joule effect remains less than 0.15°K, given the sensitivity of the background noise of the apparatus and this self-heating value. The accuracy of the temperature measurements may be assessed to be $\pm$ 0.2° with respect to temperature fluctuations. Measurements of the sensor response times performed using pulse techniques, lead to an assessment of the wire time constant between 500 and 600 μs in flows at a temperature of 120°K and at a speed equal to M = 0.2, i.e a bandwidth of about 250 Hz to 300 Hz.

In current tests, this bandwidth seems to be adequate. However, if this feature proved to be inadequate, the measuring apparatus makes it possible to perform field measurements of the sensor time constant. It is then possible to correct the raw indication of the termometer to characterize the temperature fluctuations in a higher frequency range than the natural bandwidth of the wire.

In effect, by illustrating the wire with a first order model, we may express:

$$\tau \frac{dT}{dt} + T = T_f$$

where τ = time constant of the sensor
T = instantaneous temperature indicated by the sensor
T_f = instantaneous temperature of the fluid.

If we know τ, by deriving the signal T, then multiplying and adding to the signal we are able to calculate the temperature T_f in a frequency band 5 to 10 times higher than the cut-off frequency relative to the time constant of the wire, or for wires currently used, frequencies of the order of 2 kHz.

Figure 14 gives a comparison of the response time of the sheet thermocouples and of the cold wire. /10

Figures 15 and 16 show two vertical scannings of the T'3 test section. In the first case, the mean temperature, measured with a thermocouple and a platinum resistor was 108°K. The engine speed: 1,500 rpm; (M = 0.4), wire diameter: 9 μ. The probe (A) was fastened to a displacement device capable of scanning the test section vertically, whereas probe (B) was stationary in the middle of the test section and placed about 340 mm downstream from probe A. Given the scanner path, the sounding does not account for the boundary layer thickness.

Figure 18 summarizes the development of a gust recorded this time with two cold wires, one of which was used for sounding in the two previous figures.

3.23 Problems Associated with Heat Fluxes and With Wall Temperatures

Besides the Reynolds number, an essential similarities parameter is the temperature at which the model walls actually form during cyrogenic wind tunnel tests. The essential question is to estimate the impact of a deviation between this temperature and the adiabatic wall temperature corresponding to a zero heat flux.

We analyzed this problem using the test acquired at DERAT in the theoretical and calculation range for boundary layers while applying methods of calculating turbulent boundary layers developed for compressible flows with heat flux.

Method of Calculation Used

The method of calculation primarily used in these applications is an integral method which consists of solving overall equations of boundary layer momentum and energy to which an overall equation of continuity (or equation of drive) is included. Additional relationships between the various integral magnitudes of the boundary layer, required for closure, are derived from similarities solutions formed using a diagram of the mixing length. The method enables the main typical boundary layer thicknesses to be calculated (displacement thickness δ_i, momentum thickness θ, parameters in compressible and incompressible form, H and Hi, as well as the local friction factor C_f and the heat flux factor C_n.

Configurations Studied /11

Since the goal is to analyze the impact of the wall temperature as a function of the pressure gardients which may appear on two-dimensional obstacles, in applying the calculation method, we considered various distributions of the Mach number of the flow outside the boundary layer. These distributions are shown in figiure 17.

A uniform flow at M_o = 0.7 is primarily formed over a 0.4 m length.

Various distributions of the Mach number then give negative puressure gradients (-7, -5, -3), a zero gradient (0) and positive pressure gradients of variable intensity (1, 2, 3, 4, 5, 6, 7) capable of leading to a separation of the boundary layer, assumed

to be turbulent from the beginning.

The total length calculated is L = 0.86 m.

The calculations were performed for three generating pressures, P_{io} = 0.1, 1 and 10 bars, for a cyrogenic flow temperature T_{io} = 120°K.

The Reynolds numbers based on the Mach number M_o = 0.7 are respectively:

$$\frac{\rho_o V_o L}{\mu_o} = 3.82.10^6; \quad 3.82.10^7 \quad ; 3.82.10^8$$

We will more especially analyze the results relative to P_{io} = 1 bar, the Reynolds number of which is the order of magnitude of one flight Reynolds number.

To demonstrate as clearly as possible the impact of the wall temperature, our calculations included large temperature variations, considering one case of a cold wall T_p = 60°K, one adiabatic case T_p = 118.9 and two hot call cases T_p = 200°K and T_p = 250°K. The ratios of these temperatures to the adiabatic wall temperature corresponding to M_o = 0.7 are respectively:

$$\frac{T_p}{T_{f_o}} = 0.5; \quad 1; \quad 1.68; \quad 2.1$$

Results Obtained

The results for the case of an adiabatic wall (T_p = 118.9°K) for P_{io} = 1 bar, are shown in figures 18 and 19.

The variation of the dispalcement thickness and of momentum for various pressure gradients is shown in figure 18. We see very clearly the essential impact of the pressure gradient on the

thickening of the boundary layer after X - 0.4 m. The negative gradients lead to a decrease in δ_1 and in θ with respect to the case of a zero pressure gradient. The positive gradients result in a considerable increase in these thicknesses.

Figure 19 gives the incompressible parameter H_i, characteristic of the shape of the speed profile of the turbulent boundary layer, as well as the coefficient of local friction C_f. The impact of the pressure gradient is also very important, especially for positive gradients. Depending on their intensity, there is a considerable increase in the shape parameter and a definite decrease in the coefficient of friction. We are thus led to a zero coefficient of friction, namely to a separation of the boundary layer whose position advances as the pressure gradient increases.

The results on the other various wall temperature values are shown in the same way in figures 20 and 21 for T_p = 260°K, 22 and 23 for T_p = 200°K, 24 and 25 for T_p = 250°K.

Qualitatively, the observations are perfectly comparable to those made for the adiabatic case: the positive pressure gradients always result in a considerable thickening of the boundary layer and in a decrease in the coefficient of friction, namely to a separation.

Figures 26 and 27 demonstrate the impact of the wall temperature. To accomplish this, we started with a fixed abscissa, X = 0;6 mm, i.e. at about the middle of the pressure gradient part. We plotted for the various pressure gradient cases the variation in the thicknesses, in the shape parameter, and in the friction as a function of the wall temperature.

The main observations are therefore the following:

.The displacement thickness increases in all cases with the

wall temperature level. The effect increases with the pressure gradient.

The effect of the wall temperature on the momentum thickness is much smaller. The latter increases slightly with T_p/T_f for the case of intense positive pressure gradients. On the contrary it tneds to decrease when T_p/T_f increases when we switch from intense positive gradients to negative gradients.

In regard to the impact on the shape parameter of the speed profile, we see that the negative pressure gradients involve low H_i values. The impact of the wall temperature is too low. It increases only for intense positive gradients resulting in speed profiles and shape parameters which are close to those of a separation.

The impact on the friction coefficient is very clear: an increase in T_p/T_f leads in all cases to a decrease in C_f, which considerably increases the tendency for separation. /13

Figure 28 shows simultaneously the impact of three parameters: pressure gradient, wall temperature and pressure (or Reynolds number) on the separation of a turbulent boundary layer.

We see on the distribution curves of the outside Mach number the position of the separation calculated for various wall temperatures, for P_{io} = 0.1 and 1 and 10 bars successively.

It is clear that the separation advances as the intensity of the gradient increases, and as the wall temperature increases.

We also find more advanced separations as the generating pressure decreases, a phenomenon which is obviously associated with a thicker boundary layer.

4 - SUMMARY OF THE RESULTS ACQUIRED

Phase 1: Adjustment of A Cyrogenic T'3 Wind Tunnel

Assembly and adjustment of a cyrogenic wind tunnel under continuous operation. Installation of a new compressor with its driving system made up of an overmultiplier with a 3.8 ratio and a direct current engine of 125 KW. Designed for regulating the engine speed between 0 and 3,000 rotations per minute.

Study of compressor performance.

Adaptation of test section to achieve transonic speeds in the temperature range of about 120°K.

Feasibility testing of the various insulators and glues which should hold at low temperatures.

Phase 2: Experimental Technique and Adjusting Instrumentation for a Cyrogenic Environment

Comparison of various heat sensors to determine the response time. Study of temperature fluctuations near 120°K.

Sensor calibration. Verification of bandwidths of about 250 to 300 Hz.

Phase 3: Problems Associated with H at Fluxes and With Wall Temperatures /14

Analysis of the problem of the main parameters characterizing the boundary lyaer, namely: displacement thickness, momentum thickness, shape parameter, friction coefficient and heat flux coefficient as a function of the various pressure gradients and of the various temperature ratios T_p/T_{fo}. Considerable impact of positive

pressure gradients on the boundary layer and displacement thicknesses as well as on the shape parameter and on the friction coefficient.

Increase in the displacement thickness with the temperature level.

Considerable increase in the shape parameter for intense positive pressure gradients up to values near separation.

Decrease in the friction coefficient with an increase in the ratio of T_p/T_f.

5 - CONCLUSIONS

Although it operates differently than a wind tunnel with conventional gust, we were able to show that a wind tunnel under continuous operation makes it possible to study and solve many problems which arise when building a wind tunnel operating at very low temperatures. The availability of the driving energy also allows very rapid variations in the test generating conditions, such as the Mach number, pressure or temperature. The graident of the rotation speed of the compressor depends only on the mechnical strength of the compressor and on its multiplier. The variation in the engine speed is virtually instantaneous.

Inside insulation makes it possible to quickly vary the temperature levels by varying the liquid nitrogen injection rate which is not required to also cool the outside wall of the wind tunnel, for example. As it is made entirely of stainless steel, a continous operation is possible.

The installation of a compressor ofr temperatures of about 120°K shows us that a construction in aluminum alloy holds well despite the high temperature gradients it undergoes during the various tests.

A comparative study of several temperature probes, such as a thermocouple, resistance probes, a sheet thermocouple and cold wires enabled us to determine their response time. Use of a cold wire with a diameter of 9 μ is very useful for measruing temperature fluctuations up to frequencies of the order of 250 to 300 Hz.

The first theoretical calculations of the variation of the /15
various parameters characterizing a boundary layer as a function of the ratio of the Temperatures T_p/T_{fo} for negative and positive pressure gradients make it possible to predict tendencies for these parameters to increase or decrease.

6 - FUTURE PROSPECTS

The first adjustment tests on the cyrogenic wind tunnel under continuous operation and using liquid nitrogen injection into the aerodyanmic circuit has shown the good performance of the system and the feasibility of testing and determining the various parameters to characterize a transonic flow at low temperatures.

The installation of a very simple model should allow us to check a certain number of theoretical calculations performed as of now. The feasibility of a rapid variation in the rotation speed of the compressor, in conjunction with an increase or decrease in the injection of liquid nitrogen into the circuit should permit a very broad variation in the parameters. A data acquisition system which is highly performing during the assembly will facilitate this operation.

An increase in the capacity of the liquid nitrogen tank stored at a pressure of 12 bars, also makes it possible to increase the speeds in the test section while the wind tunnel is operating under pressure.

At the same time, we will continue to perfect the theoretical studies to have a better understanding of the droplet evaporation phenomenon for different storage conditions.

REFERENCES

1. Houdeville R., Cousteix J., "Two-Dimensional Turbulent Boundary Layers With Heat Flux", DERAT Technical Reports No. 3/5005, 4/5005, 5/5005, 6/5005.

2. Faulmann D., "Wind Tunnel With Injections At Low Temperatures", Technical Report No. 1/1977, Januayr 1977.

3. Faulmann D. Prieur J., Vergnolle J.F., "Preliminary Tests on a Transonic Installation Operating With Cyrogenic Gusts", 14th Symposium of Applied Aerodynamics, AAF, Toulouse, November 1977.

4. Michel R., Faulmann D., "Preliminary Tests in a Cyrogenic Transonic Wind Tunnel Driven By Injection", Spring Meeting of Supersonic Tunnel Association, El Segundo, California, USA, April 17-18, 1978, T.P. ONERA No. 1978-48 E.

5. Prieur J., Dor J.B., "Assessment of Heat Losses and Calculations of the Characteristics of Flows in a Wind Tunnel With Cyrogenic Gusts", ONERA/CERT/DERAT Technical Report No. 4/5007 AND, June 1978.

6. Blanchard A., Faulmann D., "Progress Report on a Cyrogenic Pilot Transonic Wind-Tunnel Driven by Induction", Symposium on Cyrogenic Wind Tunnels, Southampton, G.B., April 3-5, 1979.

7. Mignosi A., Archambaud J.P.", "Prediction of Thermal Losses and Transient Flows in a Cyrogenic Wind Tunnel", Symposium on Cyrogenic Wind Tunnels, Southampton, G.B., April 3-5, 1979.

LIST OF FIGURES

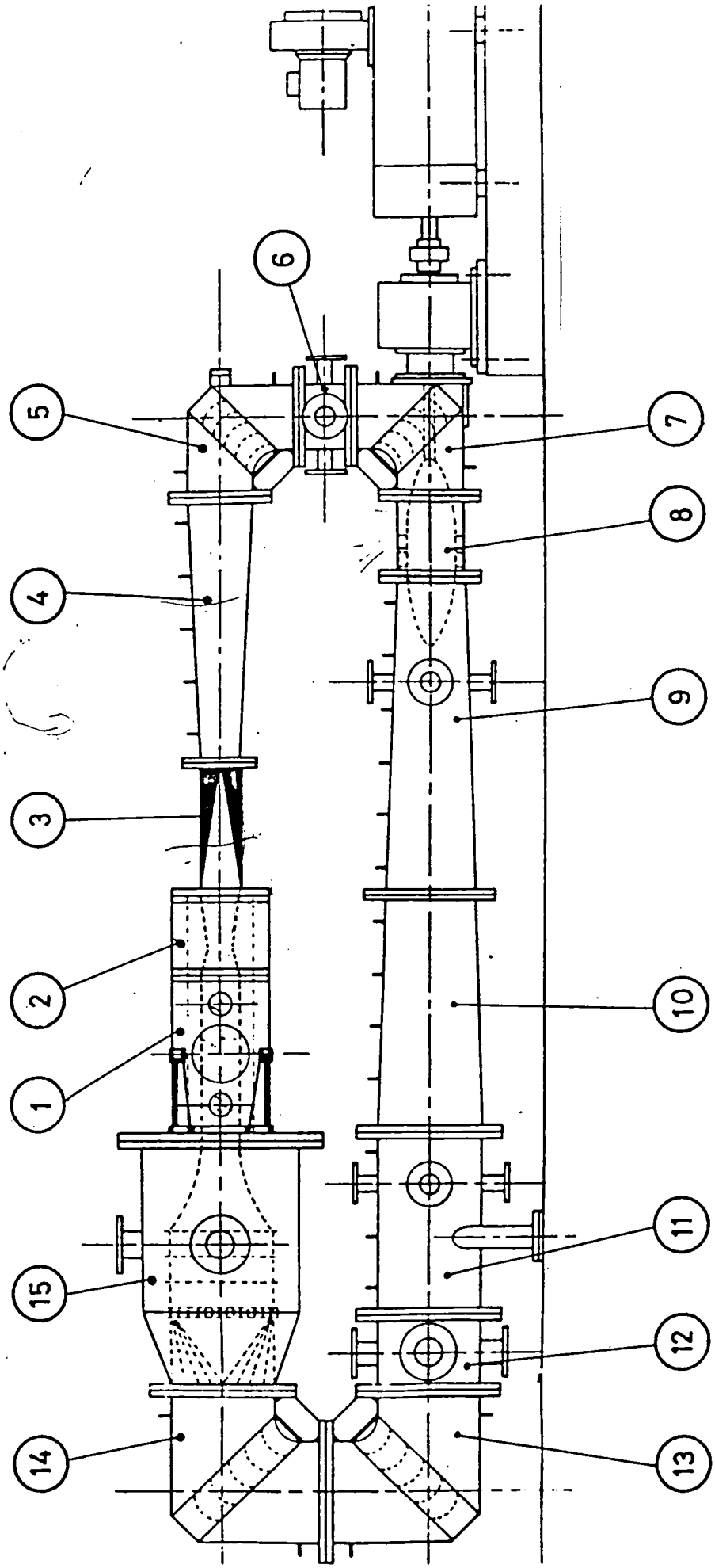

22 Figure 1 - Diagram of the T'3 Cyrogenic Wind Tunnel

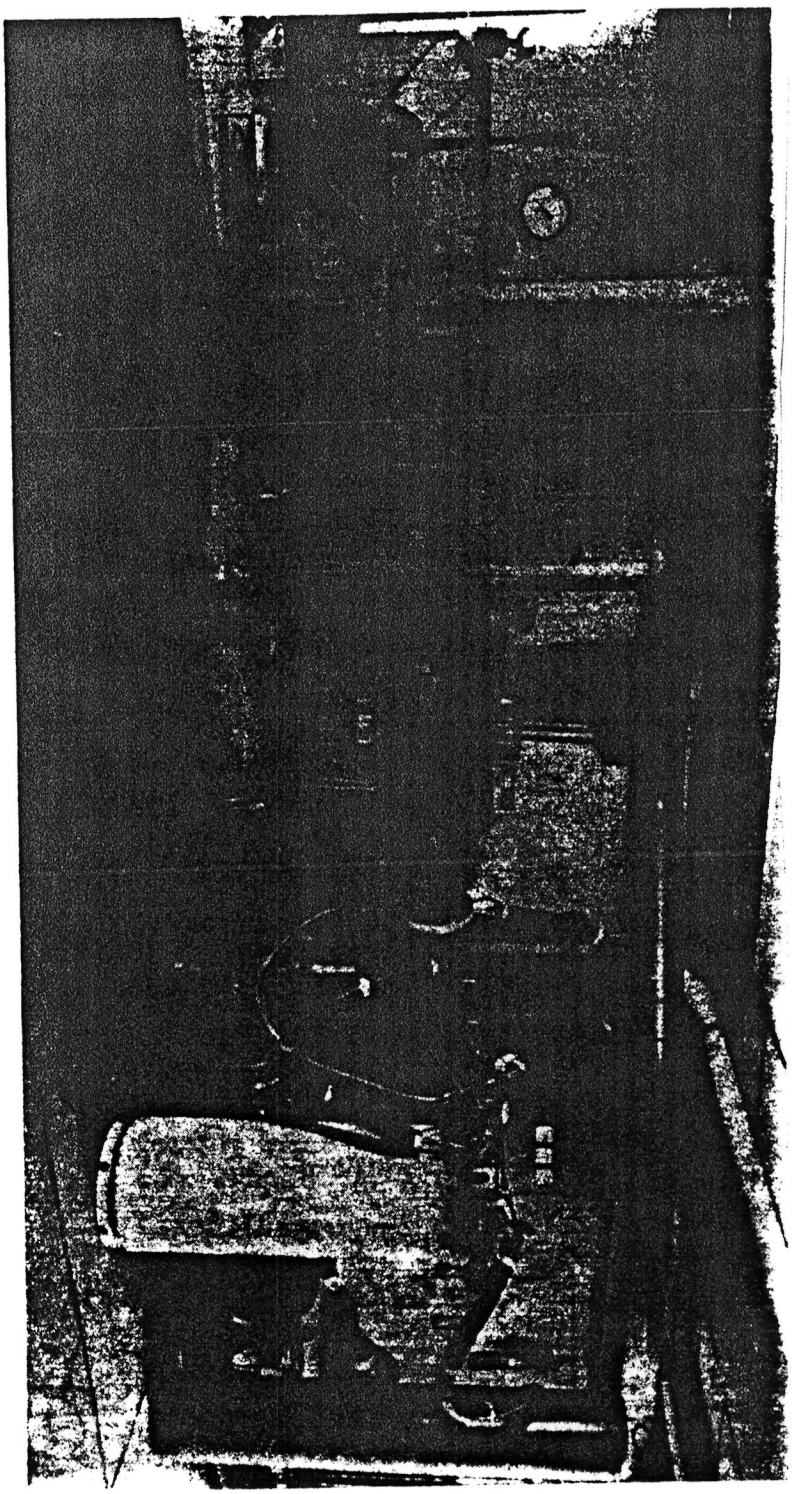

Figure 2 - The T'3 Cyrogenic Wind Tunnel

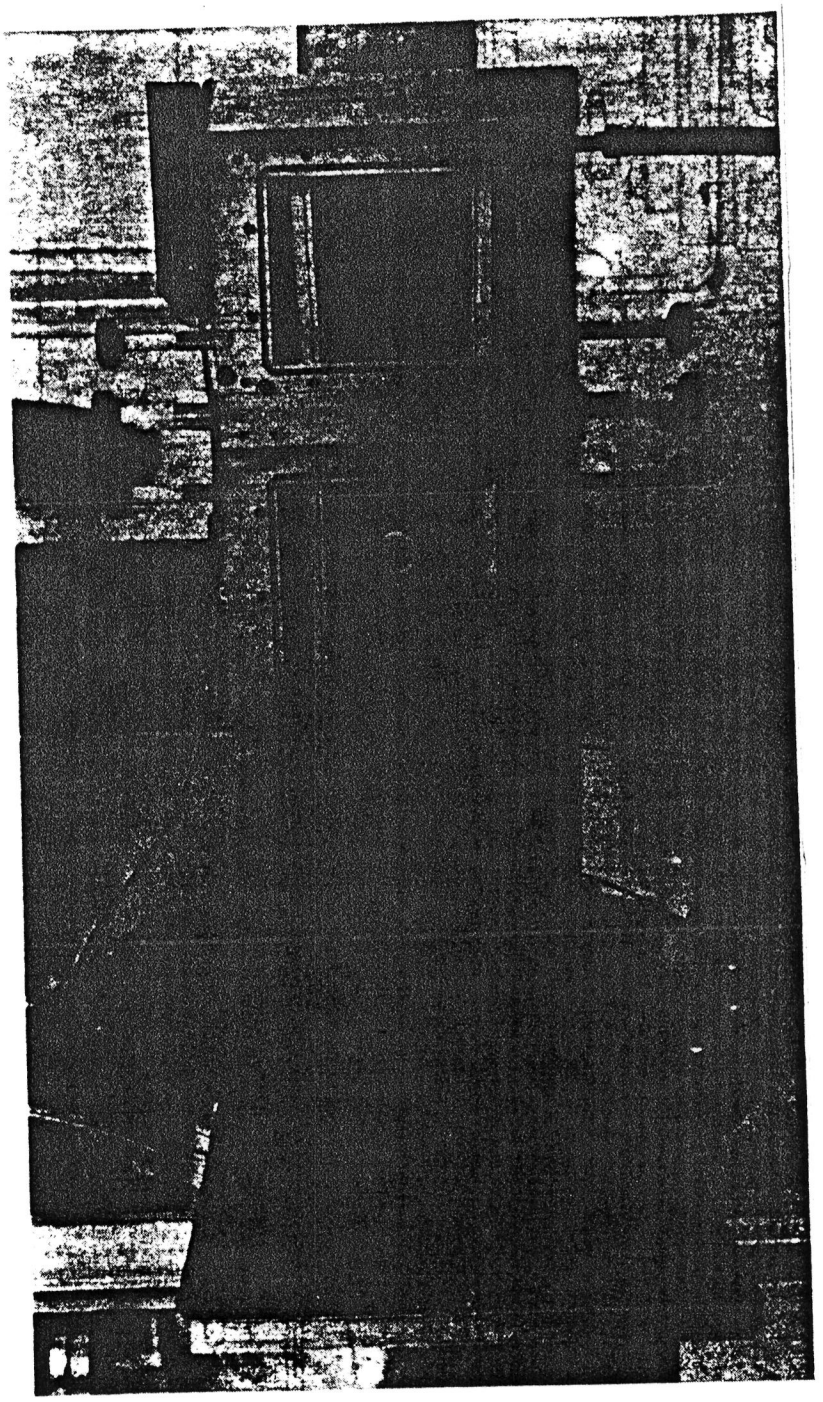

Figure 3 - Test Section and Neck Element

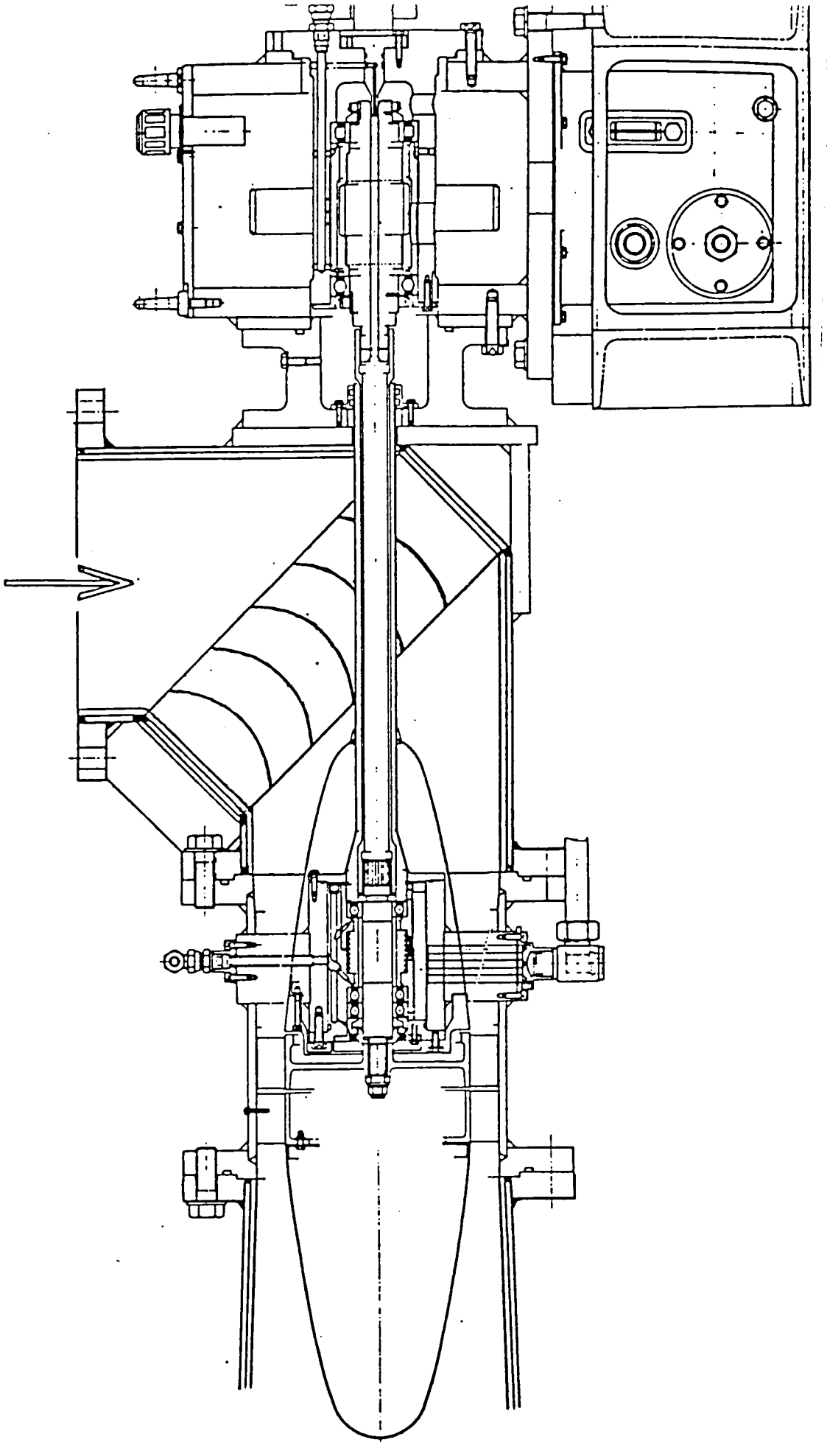

Figure 4 - Axial Compressor

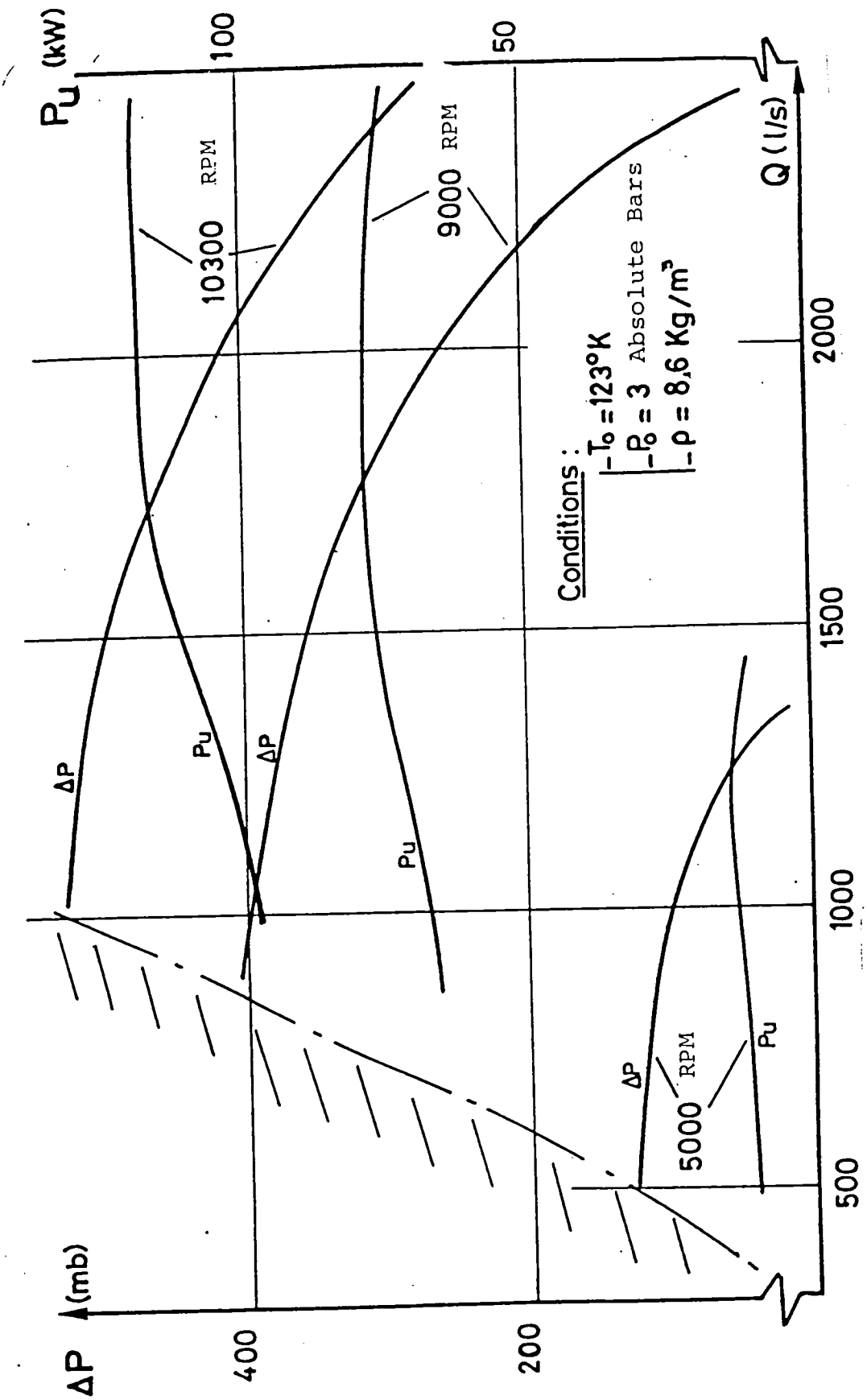

Figure 5 - Theoretical Performance of the Compressor

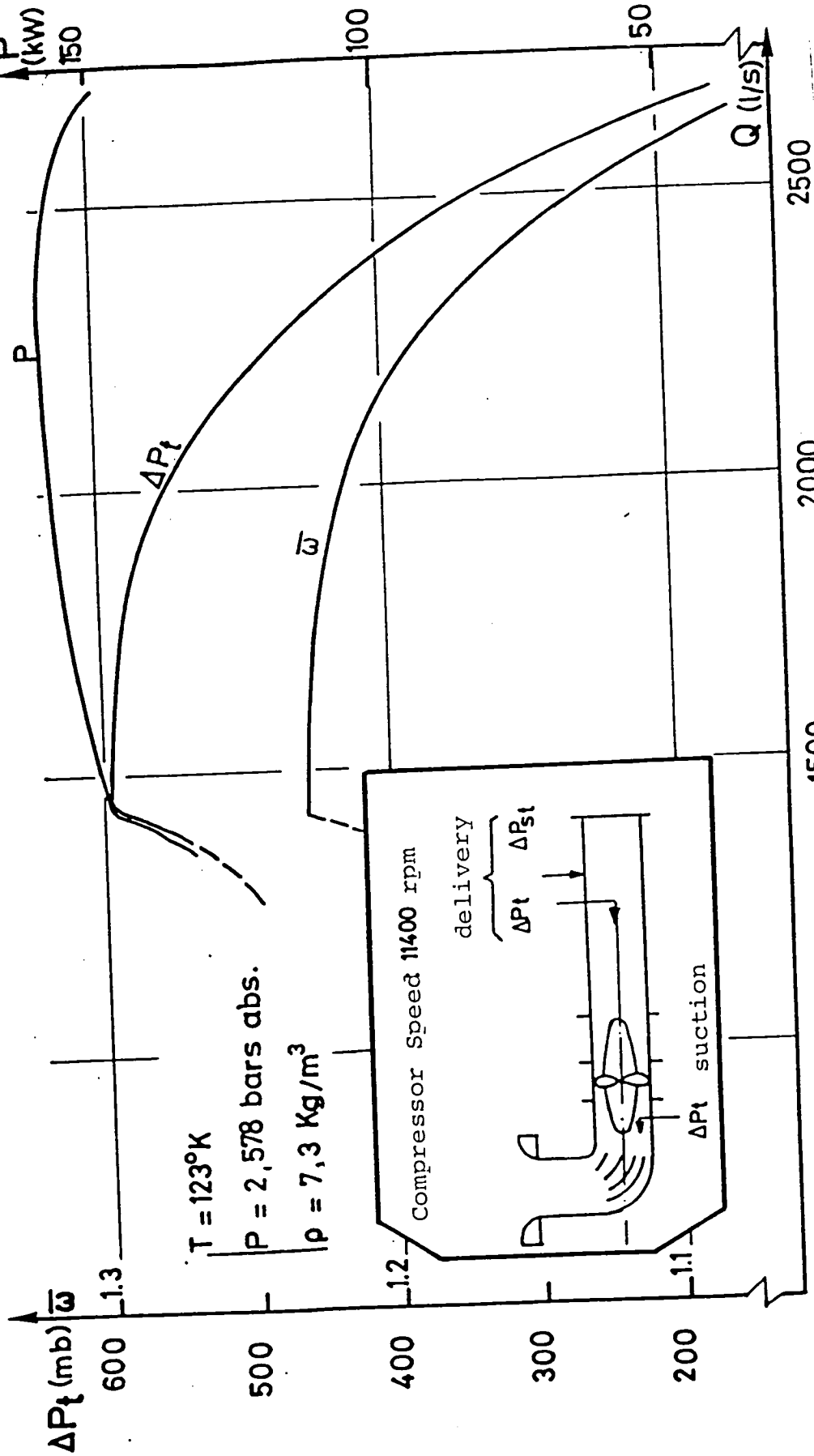

Figure 6 - Experimental Results

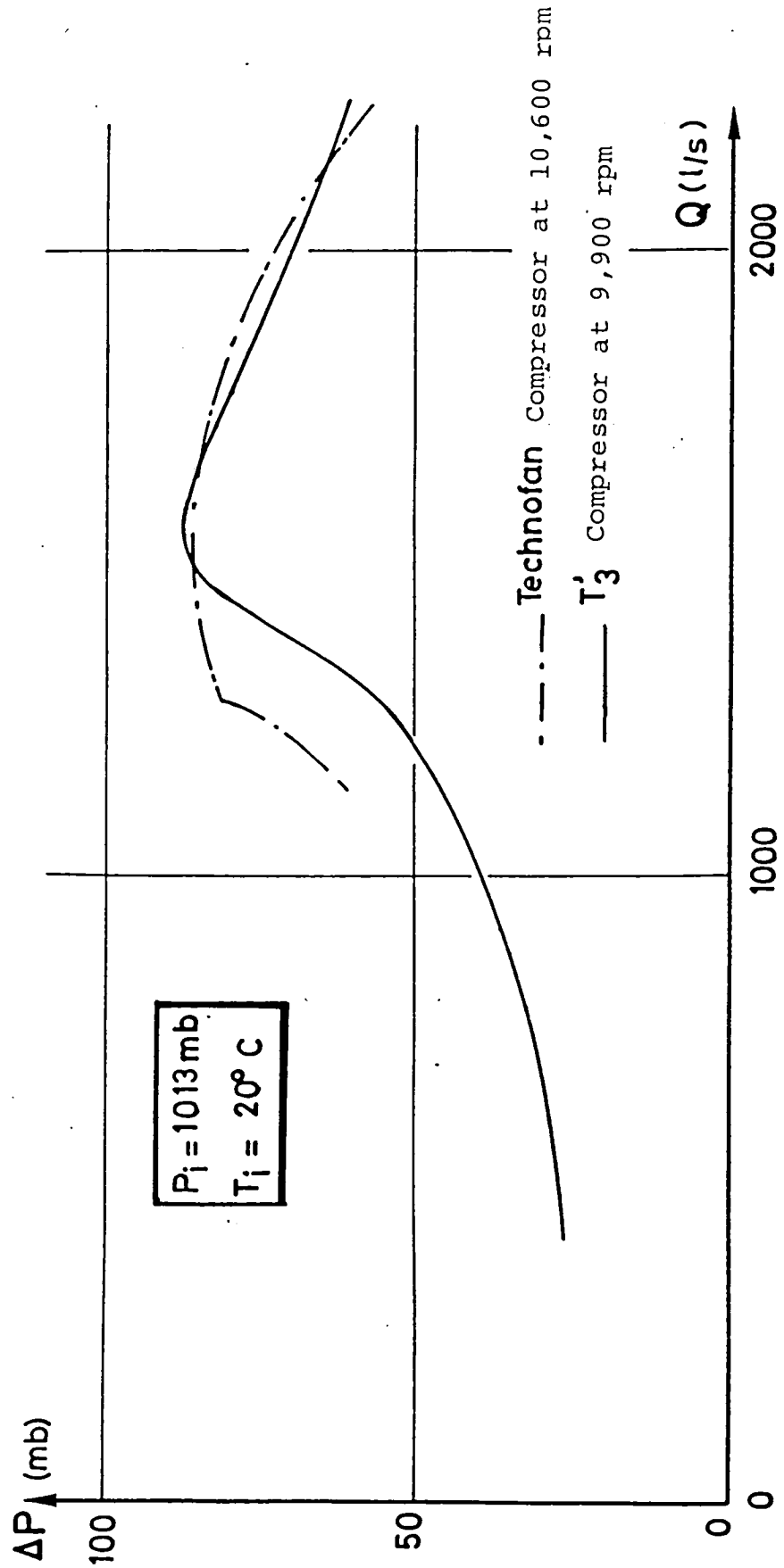

Figure 7 - Comprarison of the Two Tests

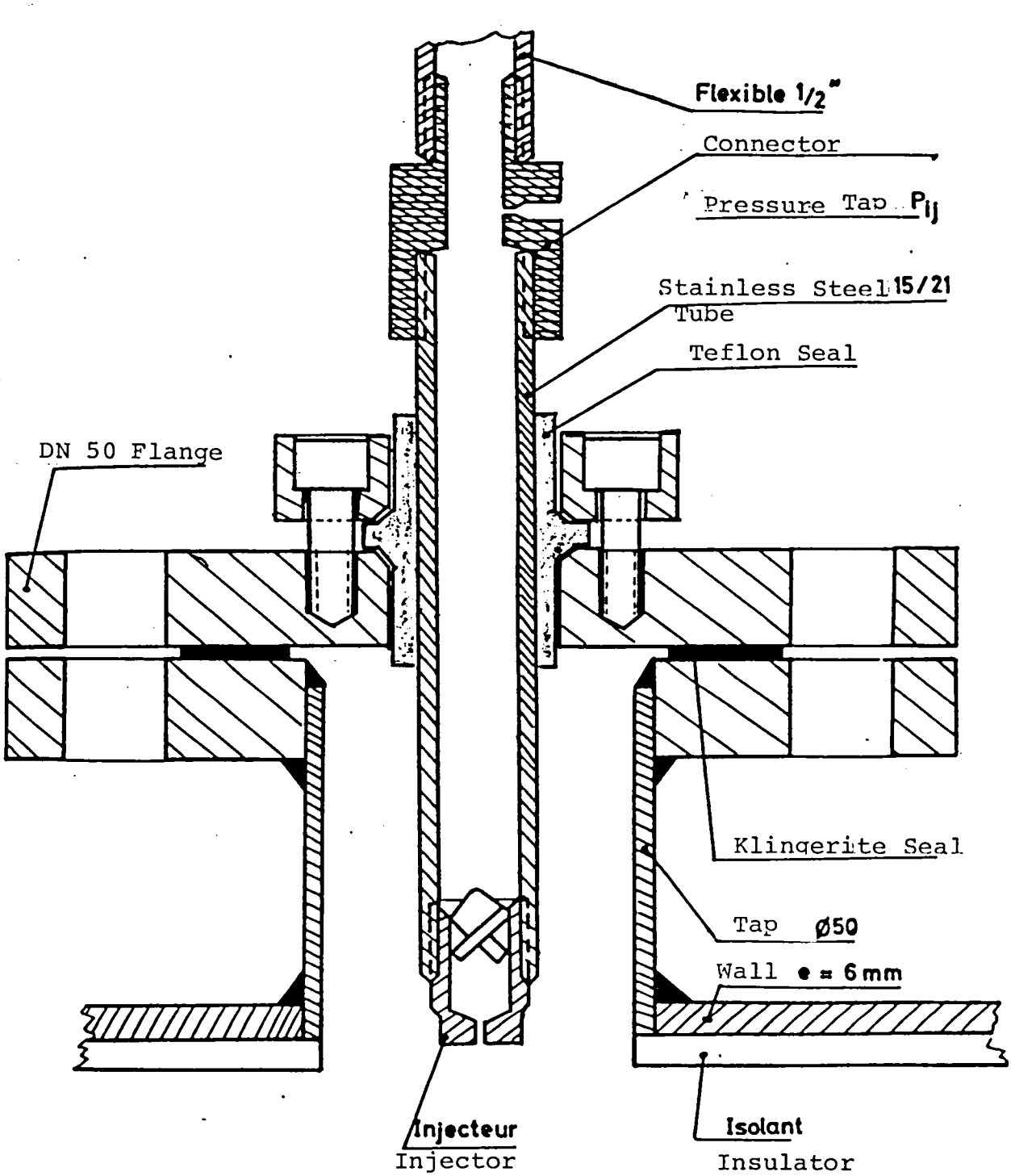

Fiugre 8 - Nitrogen Injector Installed On a NW 50 Flange.

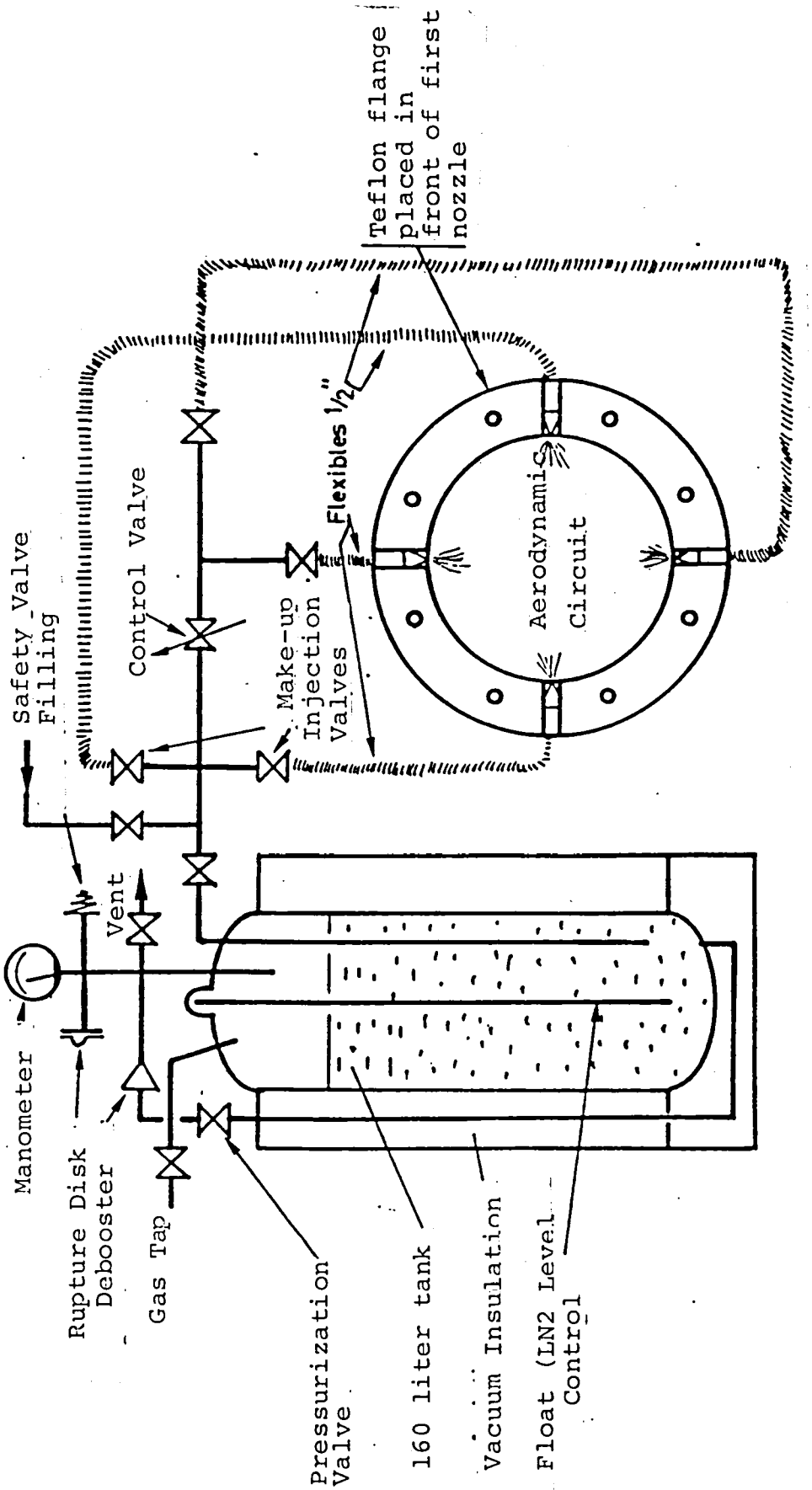

Figure 9 - Liquid Nitrogen Storage and Injection System

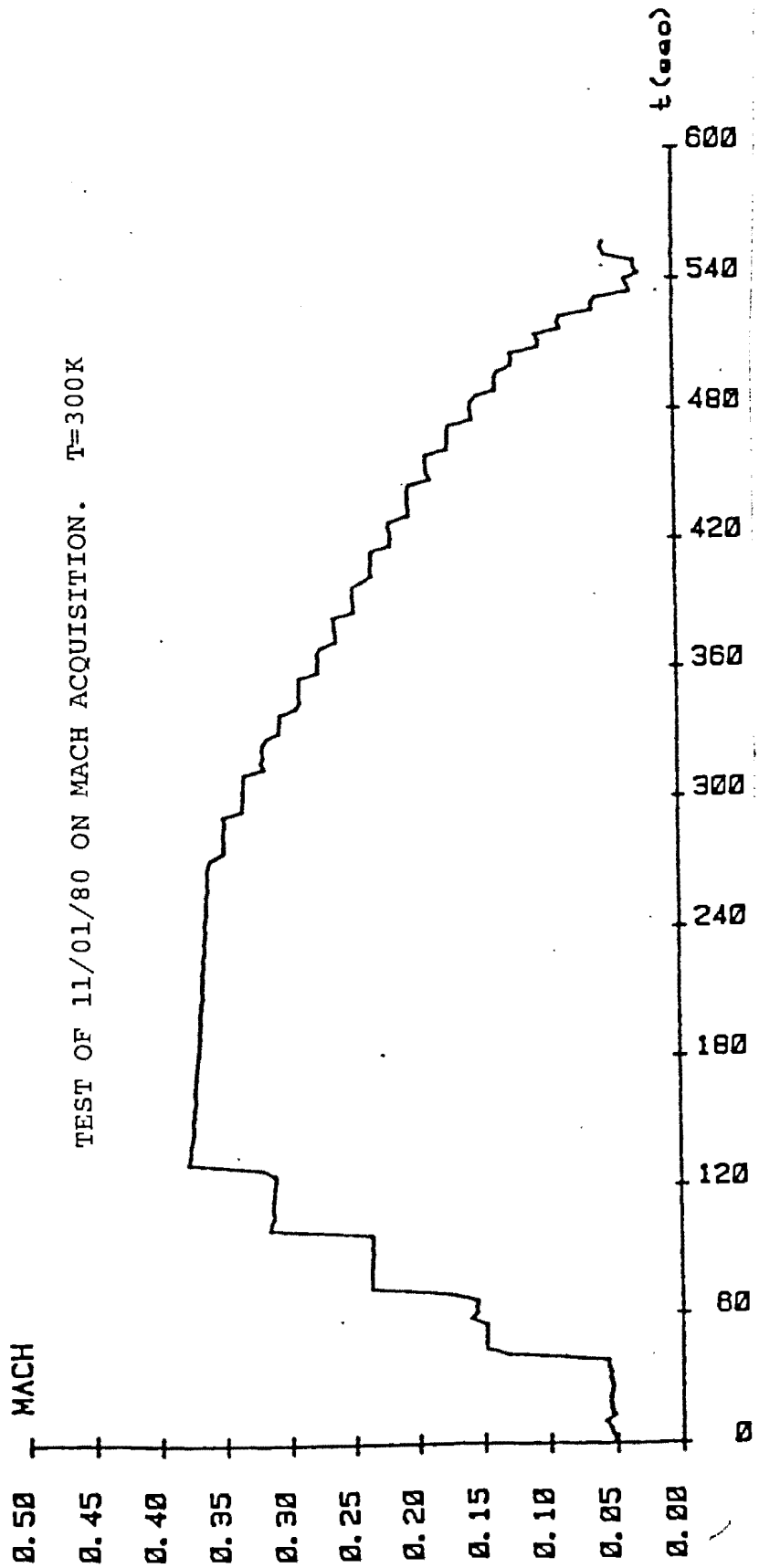

Figure 10 - Rapid Variation of the Mach Number for a Temperature of 300°K

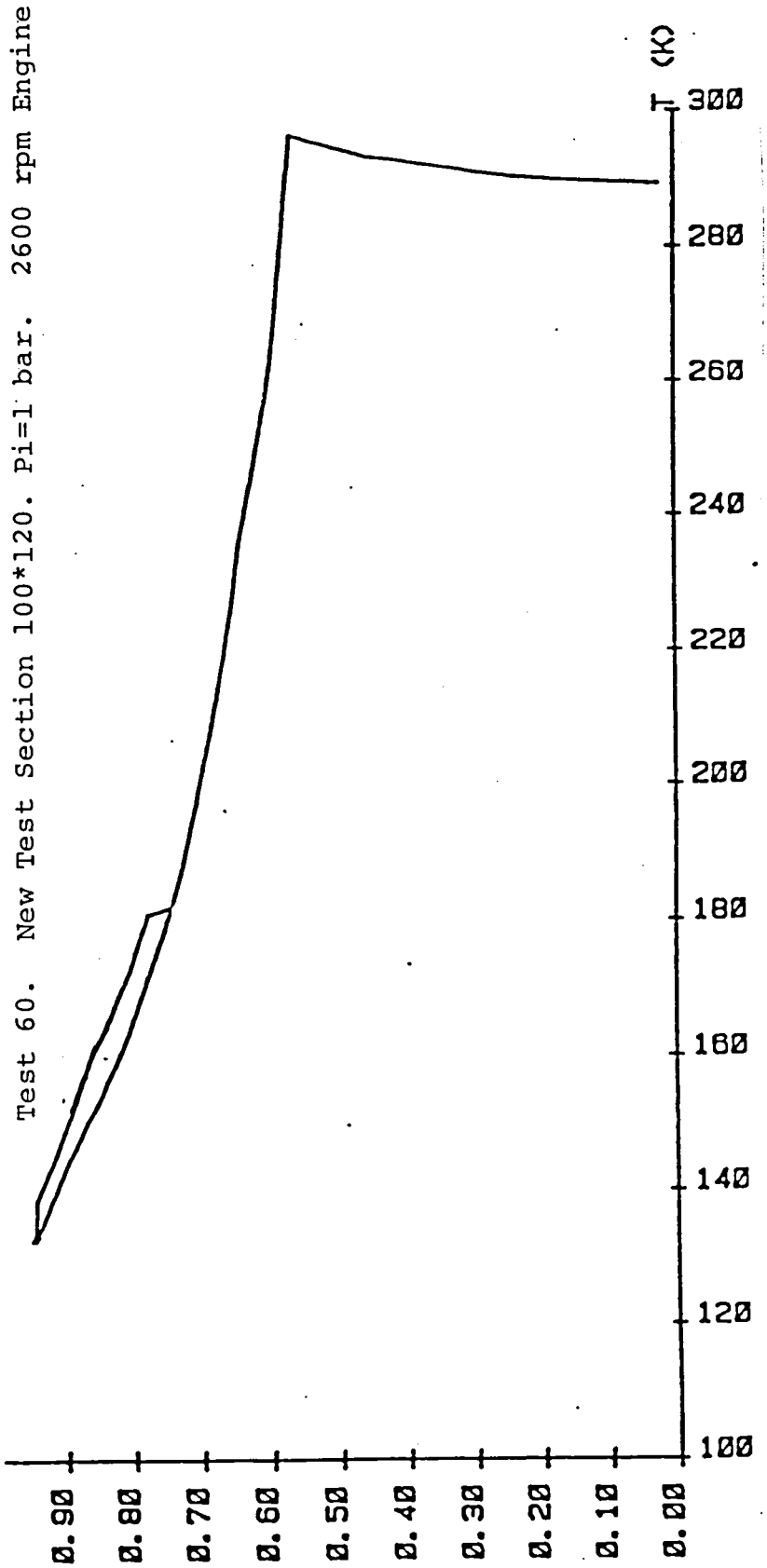

Figure 11 - Impact of Temperature on the Mach Number

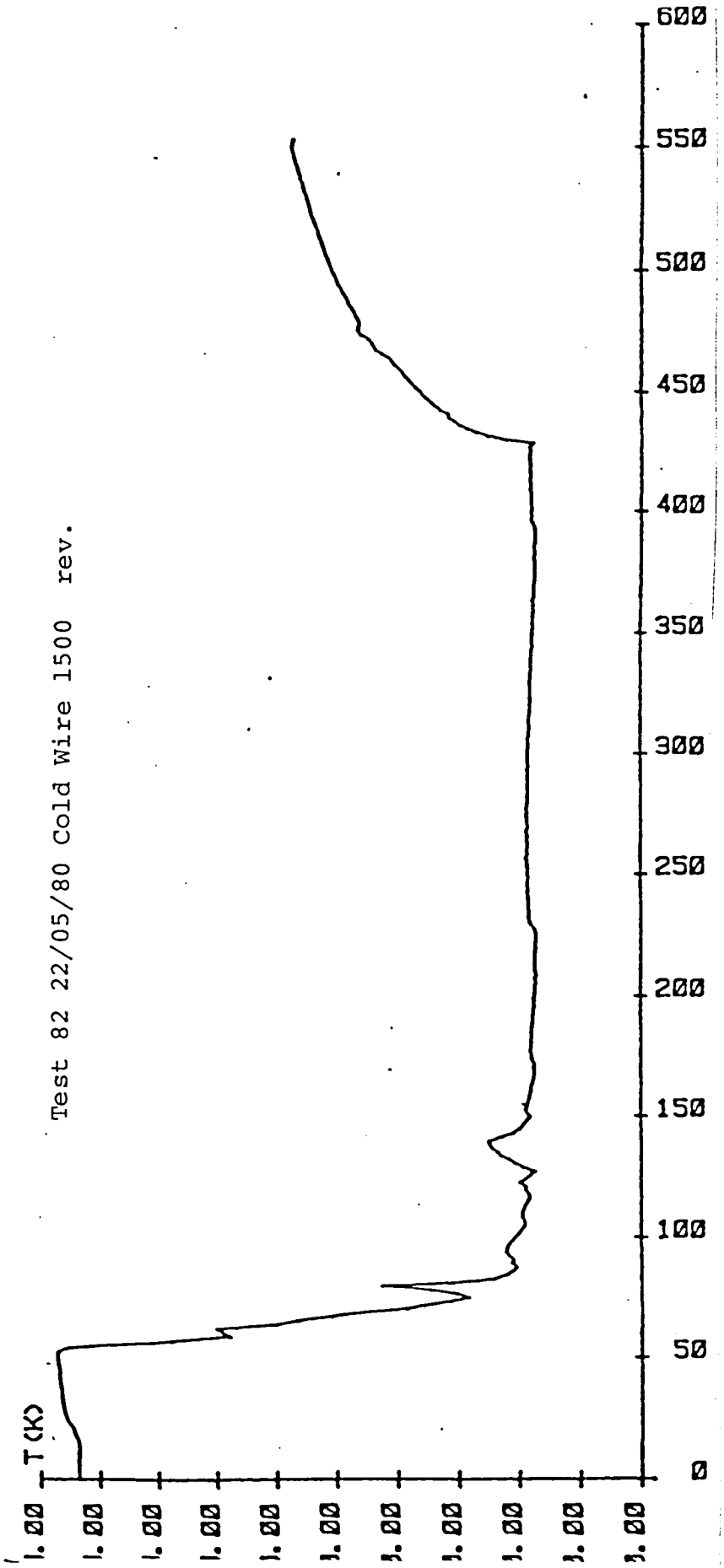

Figure 12 - Standard Test for the Study of T Fluctuations

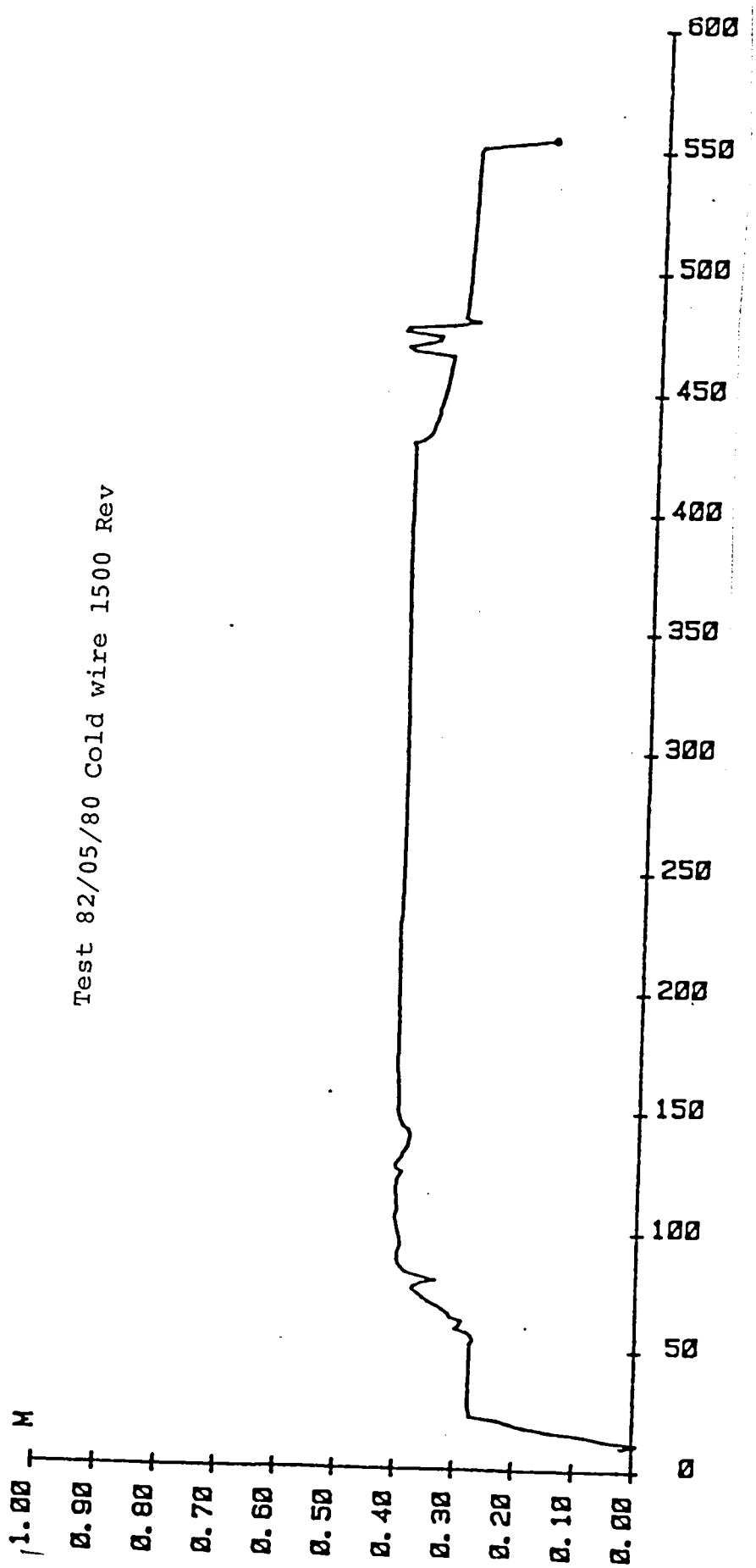

Figure 13 - Variation of Mach Number in Test Section As a Function of Time

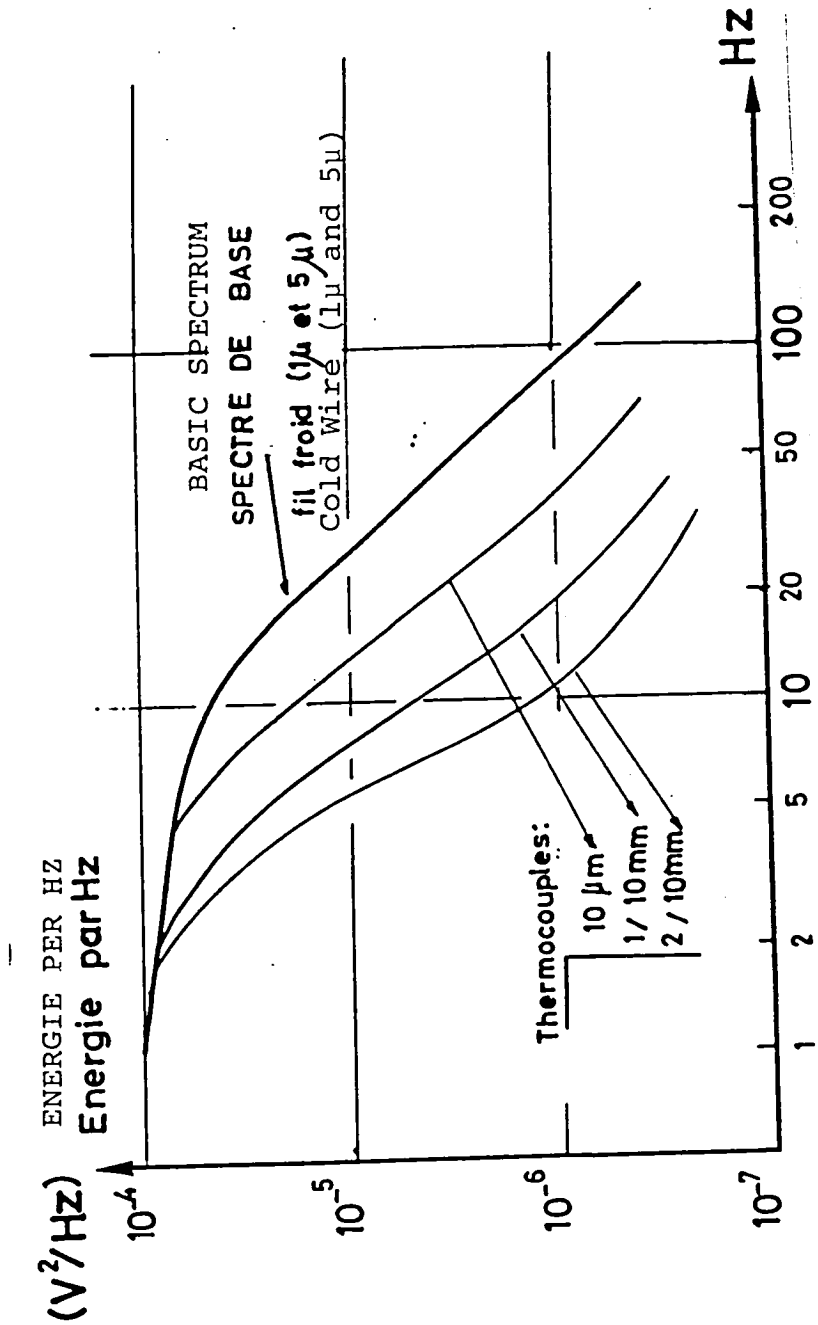

Figure 14 - Response Time of Sheet Thermocouples and of Cold Wire

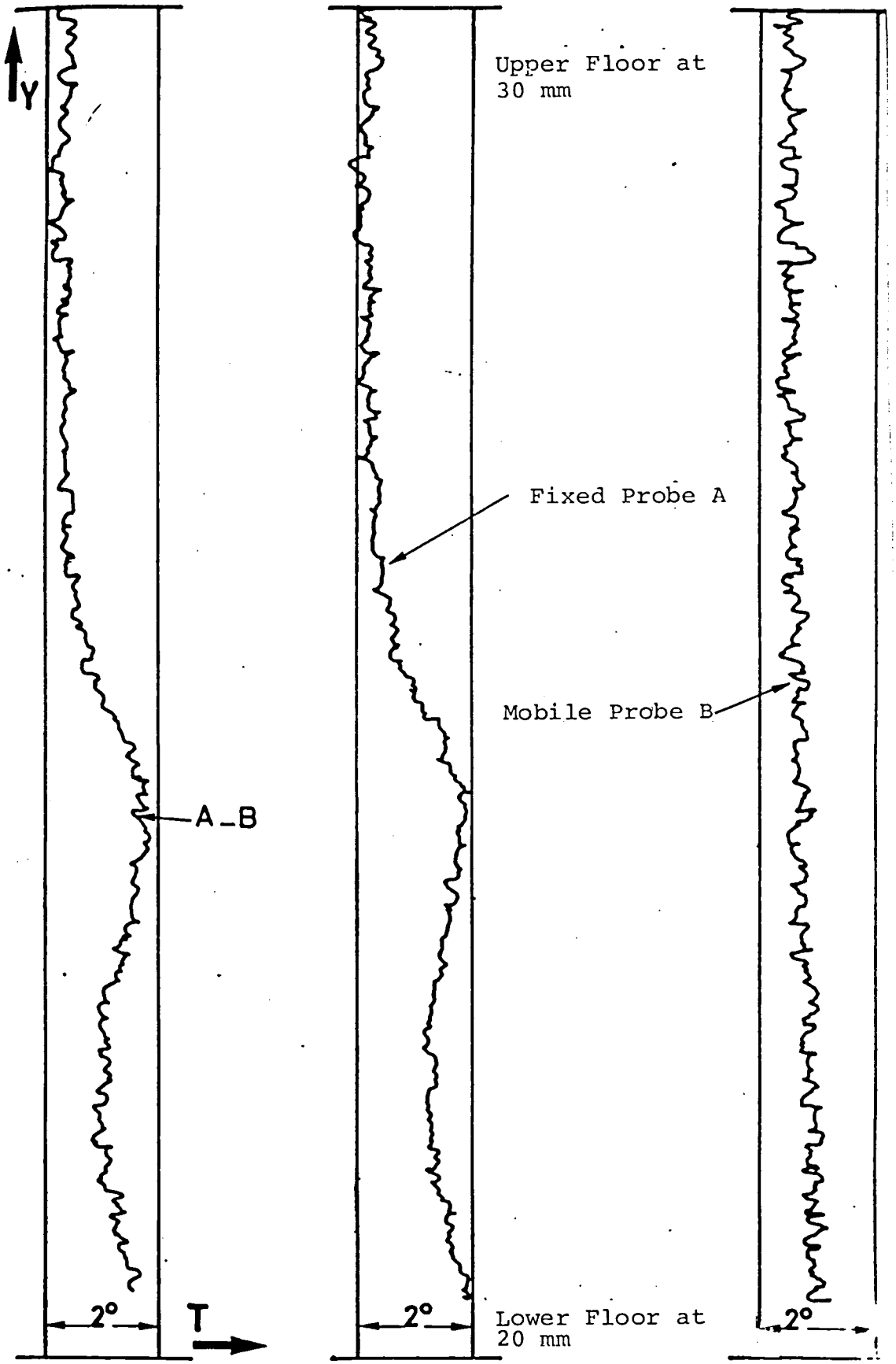

Cold Wire Test of 9 μ, T_i=108°K, Engine Speed: 1500 rpm

Figure 15 - Scanning the Test Section

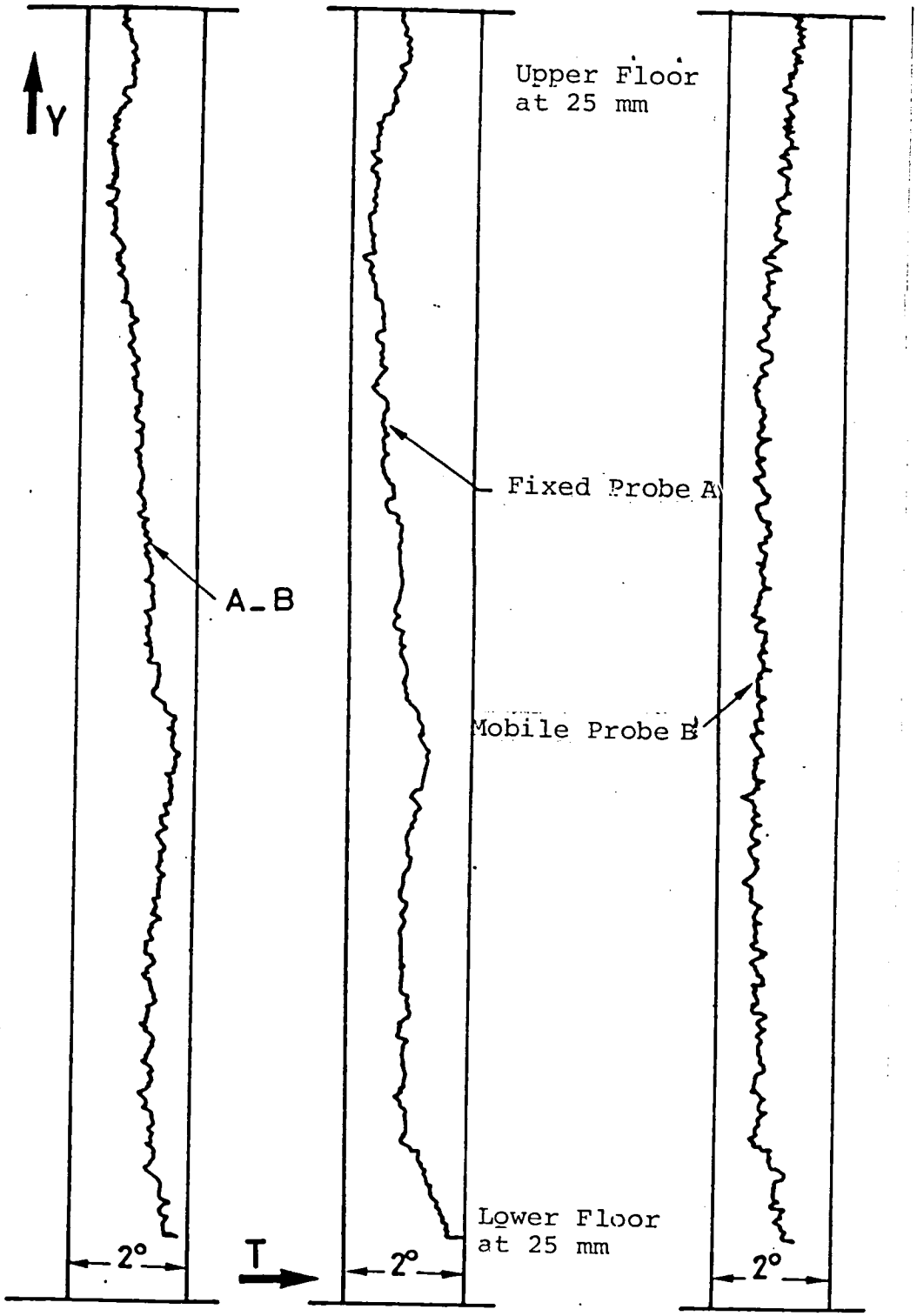

Cold Wire Test of 9μ, T_i=158°K, Engine Speed: 2000 rpm

Figure 16 - Vertical Scanning of Test Section

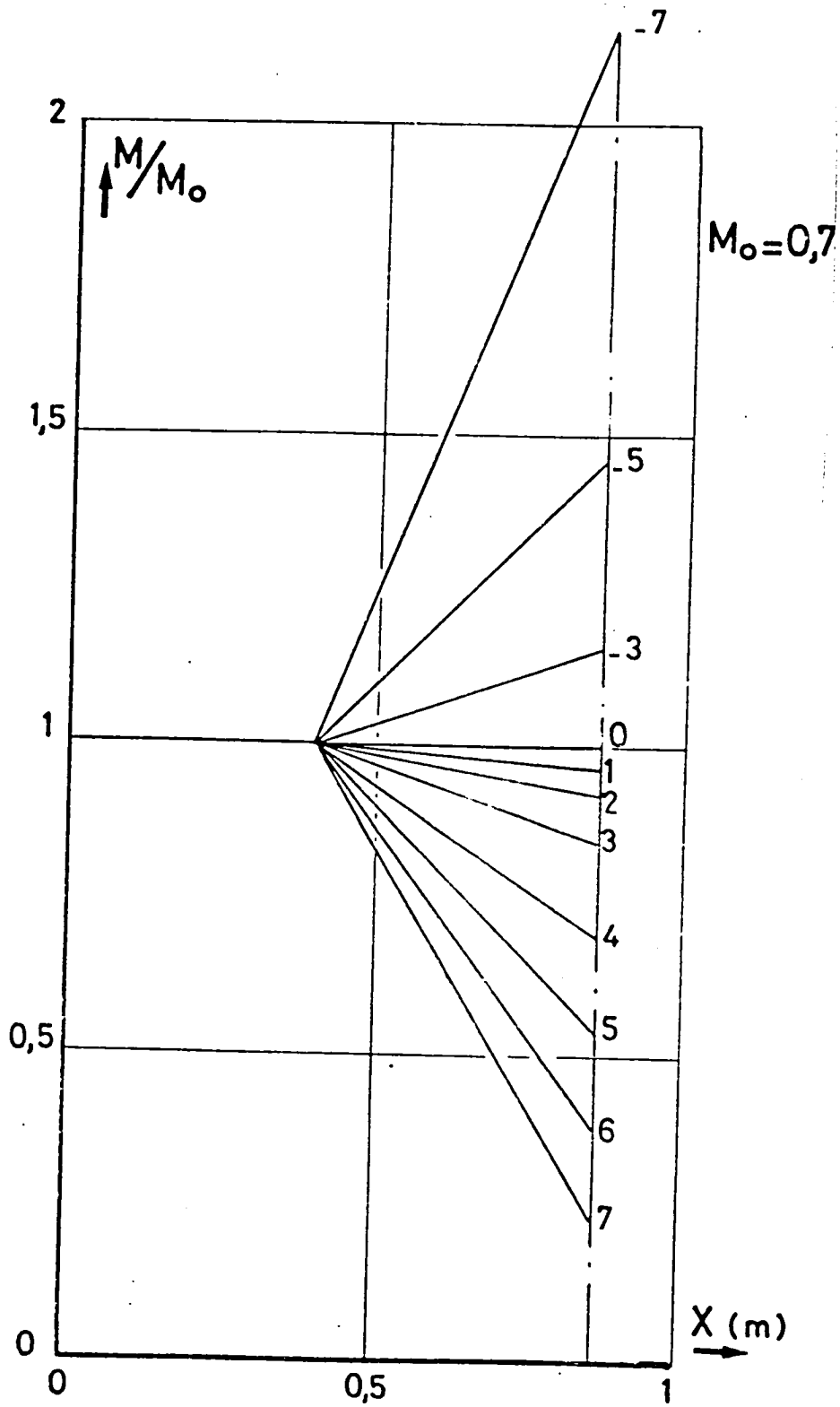

Figure 17 - M/Mo = f(x), Variable dp/dx

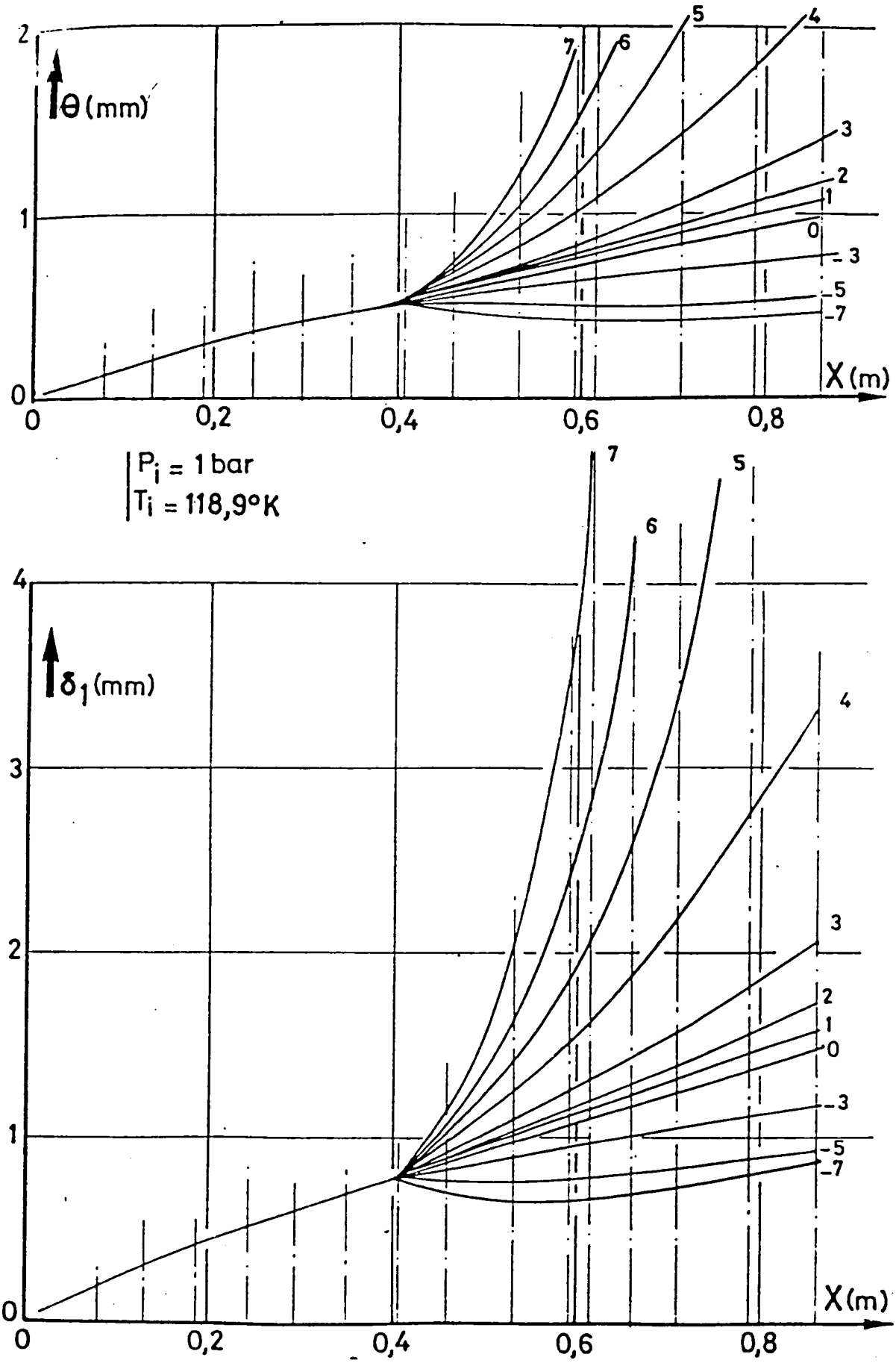

Figure 18 - θ and δ_1 = f(x), variable dp/dx

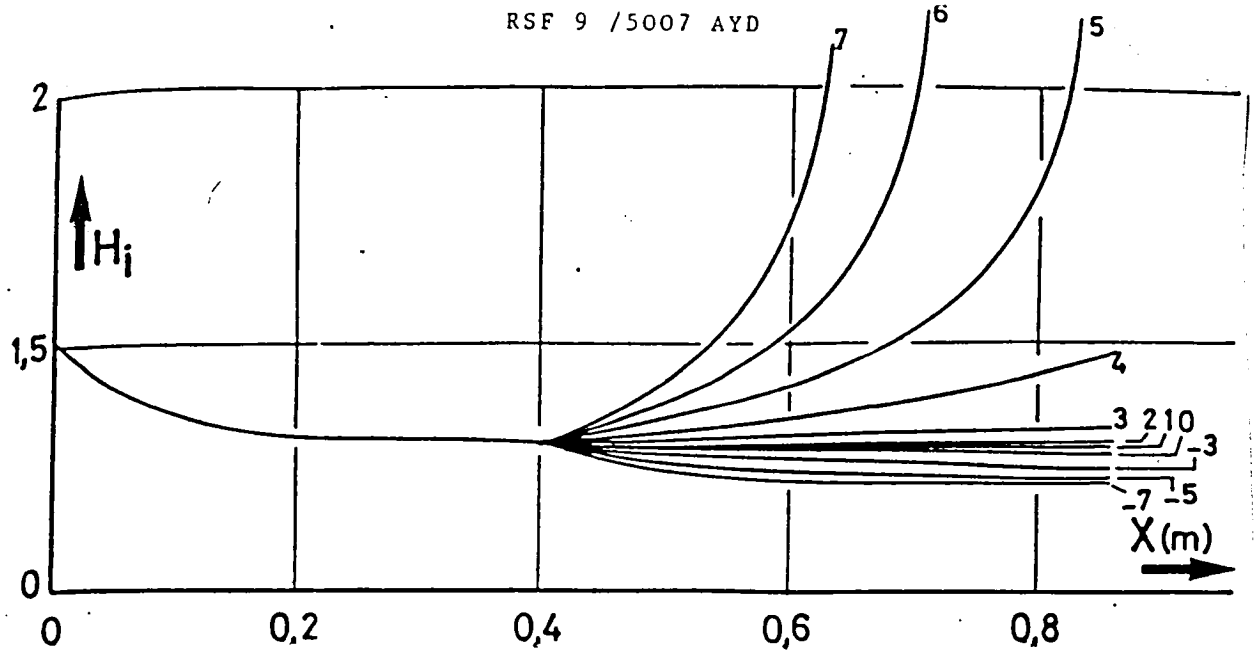

$P_i = 1$ bar
$T_i = 118.9°K$

Figure 19 - Hi and Cf = f(x), variable dp/dx.

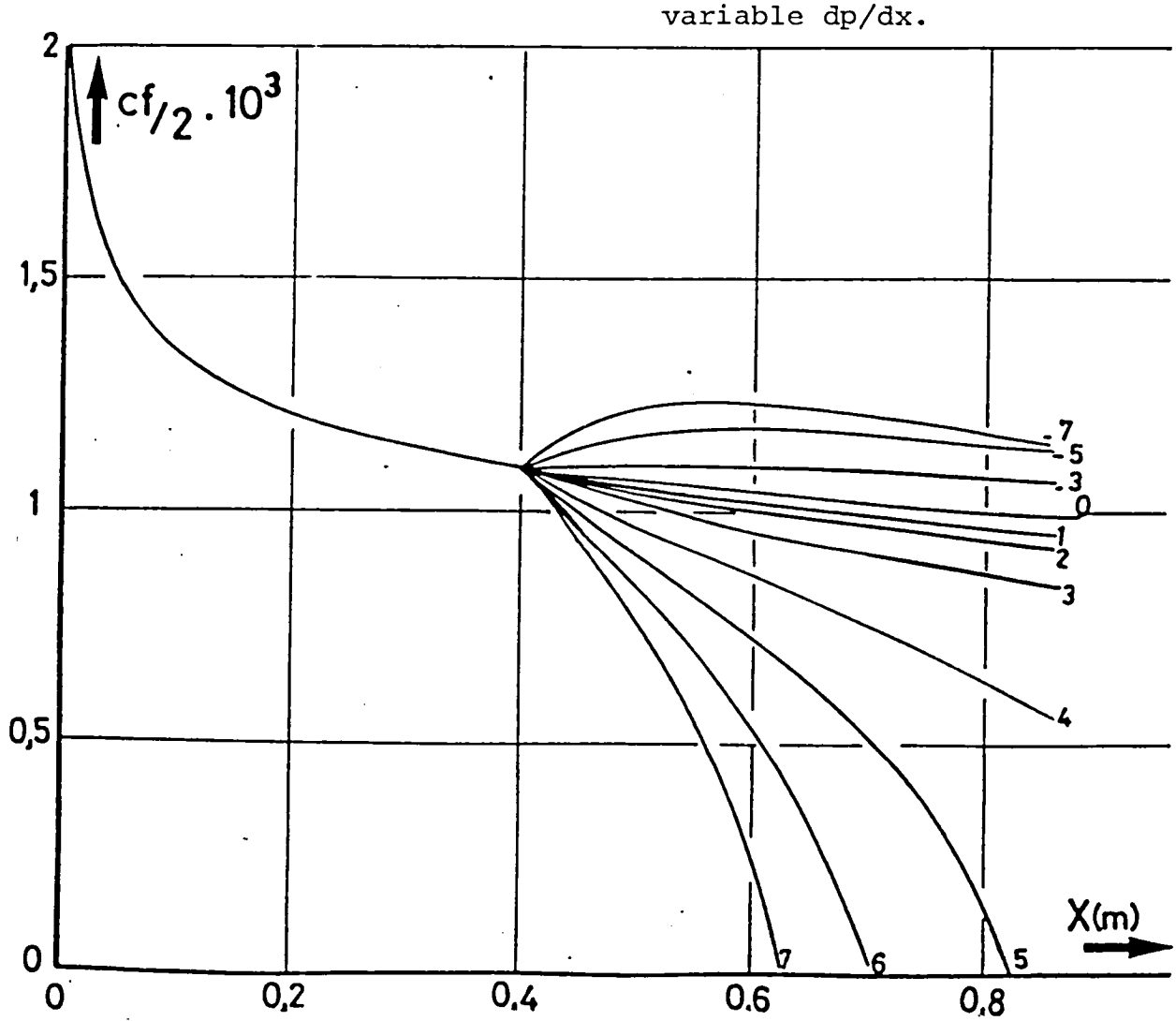

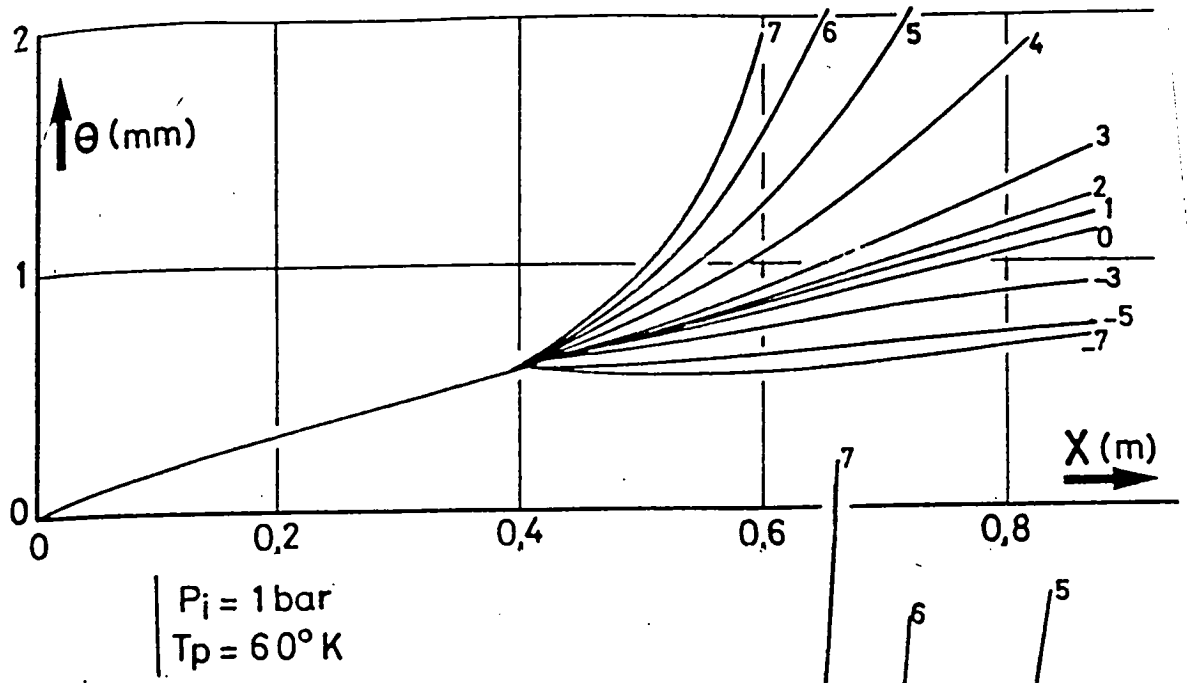

Figure 20 - θ and δ = f(x), variable dp/dx

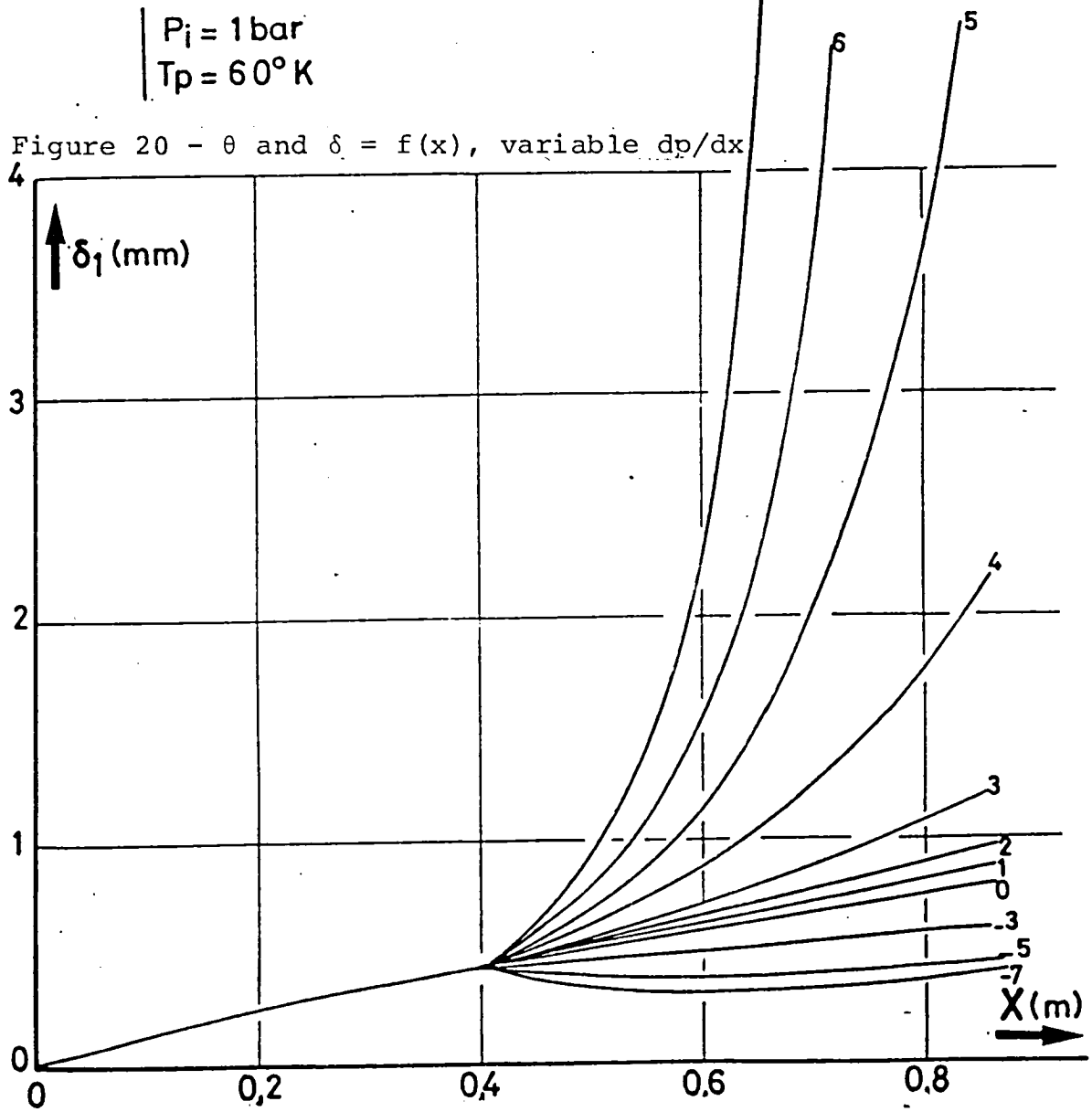

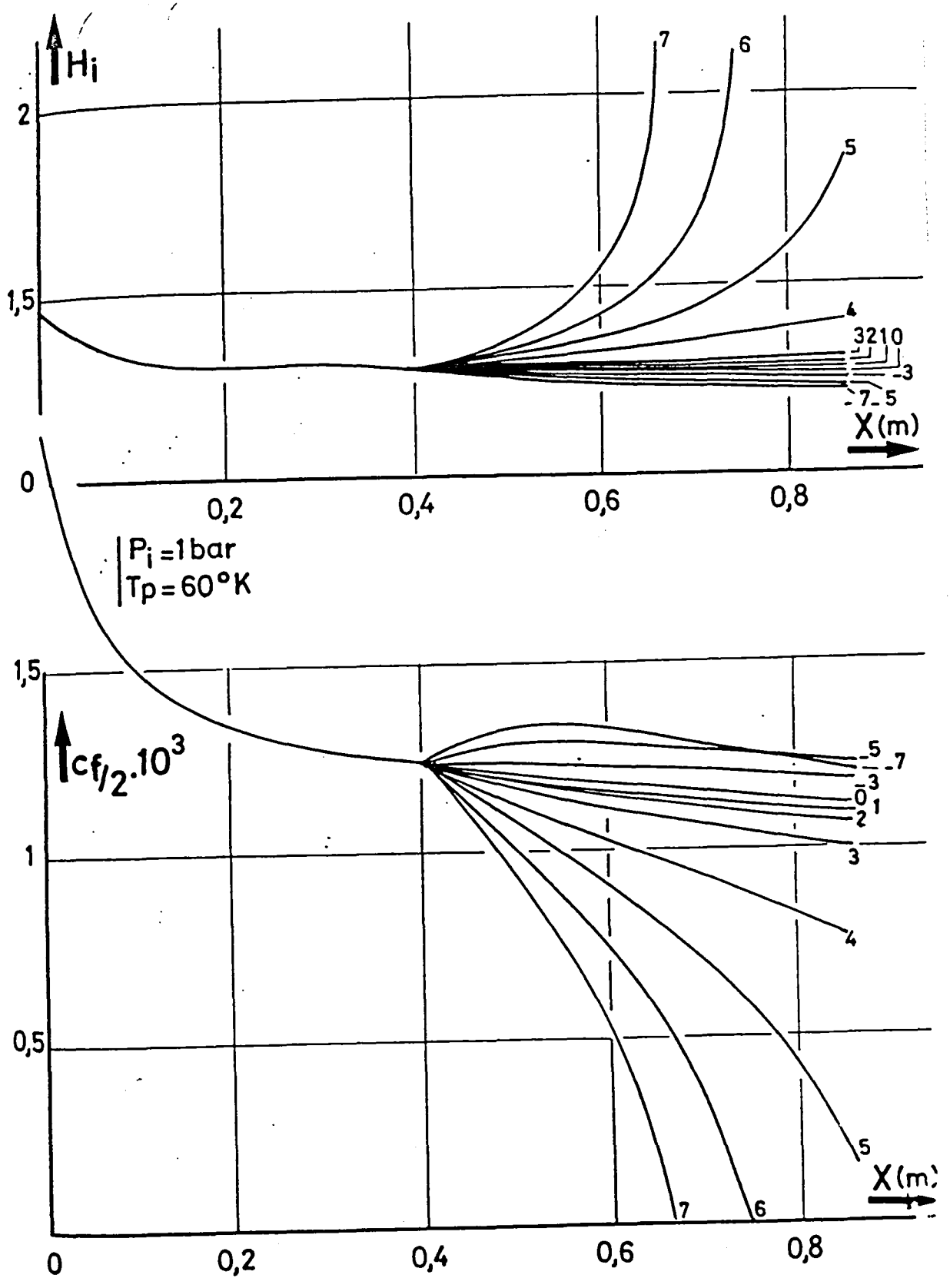

Figure 21 - Hi and Cf = f(x), variable dp/dx

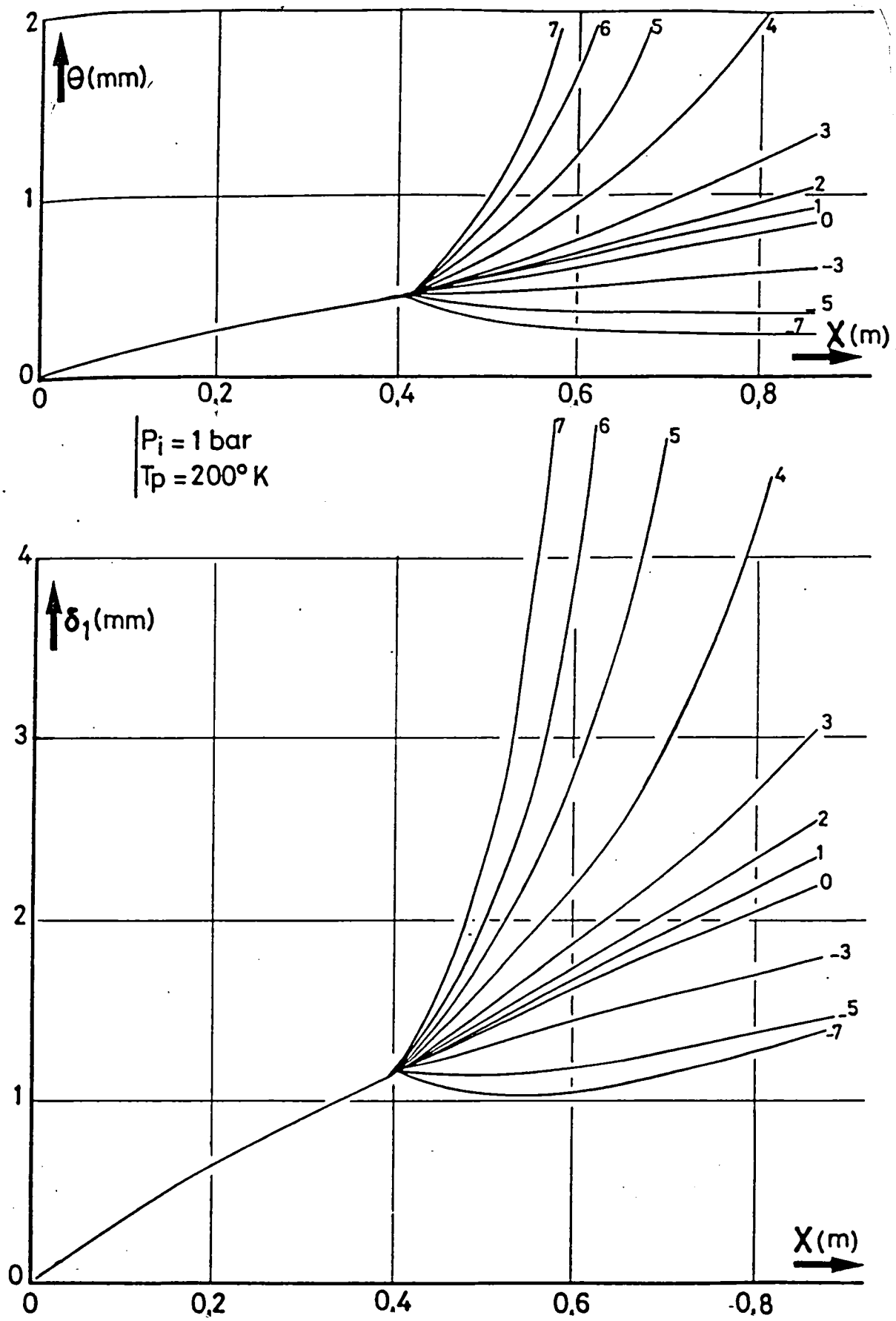

Figure 22 - θ and δ_1 = f(x), variable dp/dx

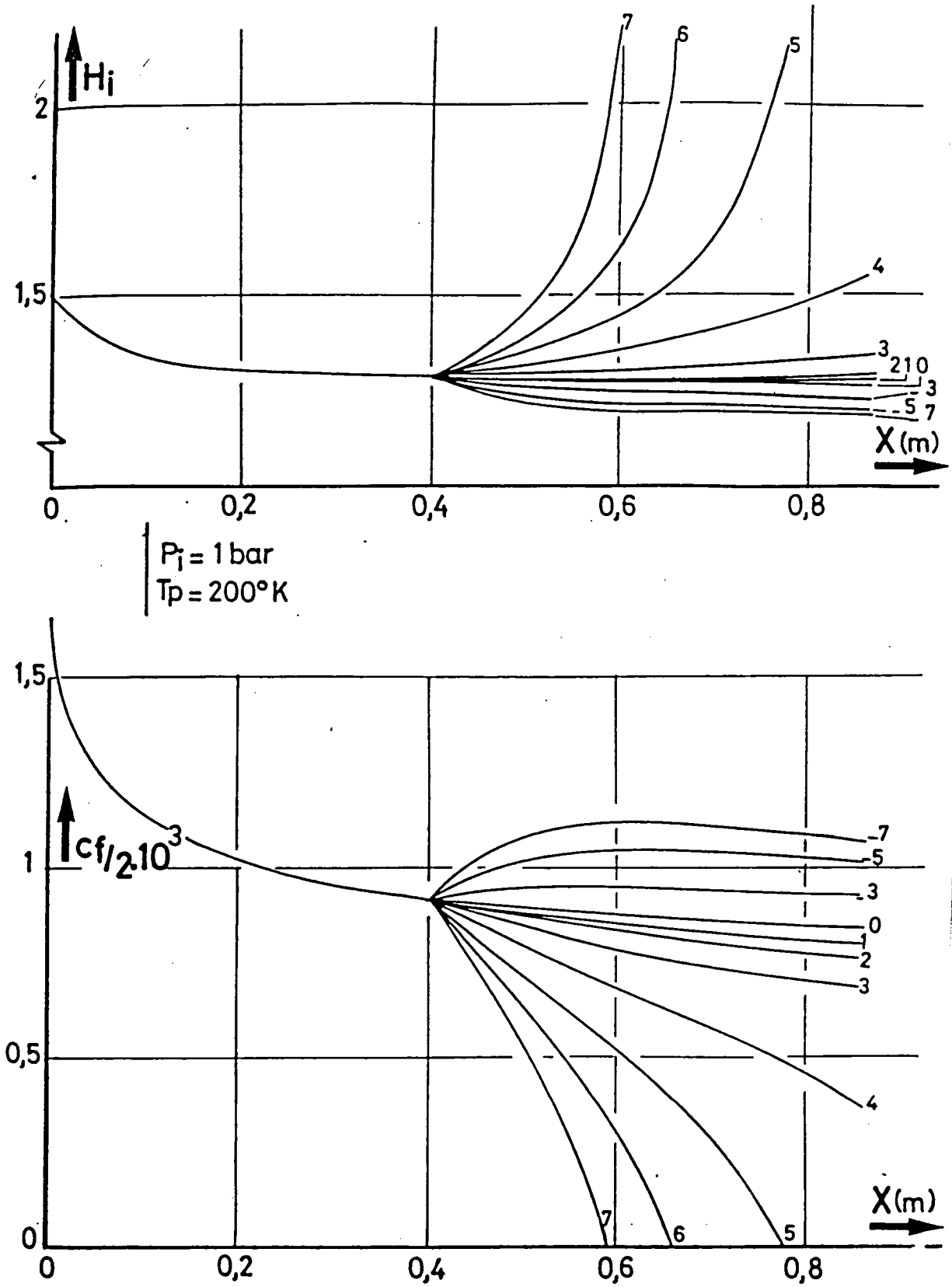

Figure 23 = Hi and Cf - f(x), variable dp/dx

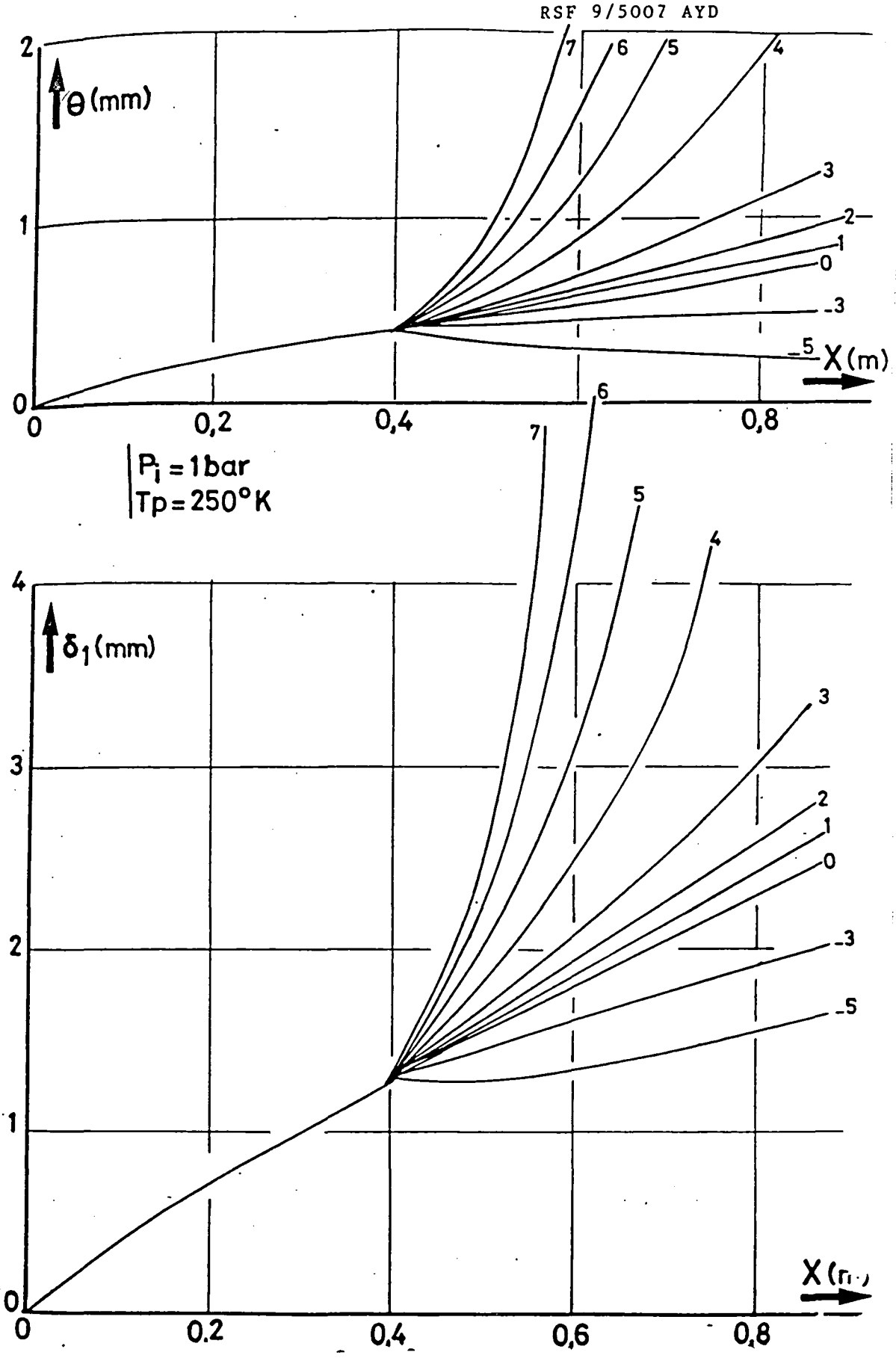

Figure 24 - θ and δ_1 = f(x), variable dp/dx

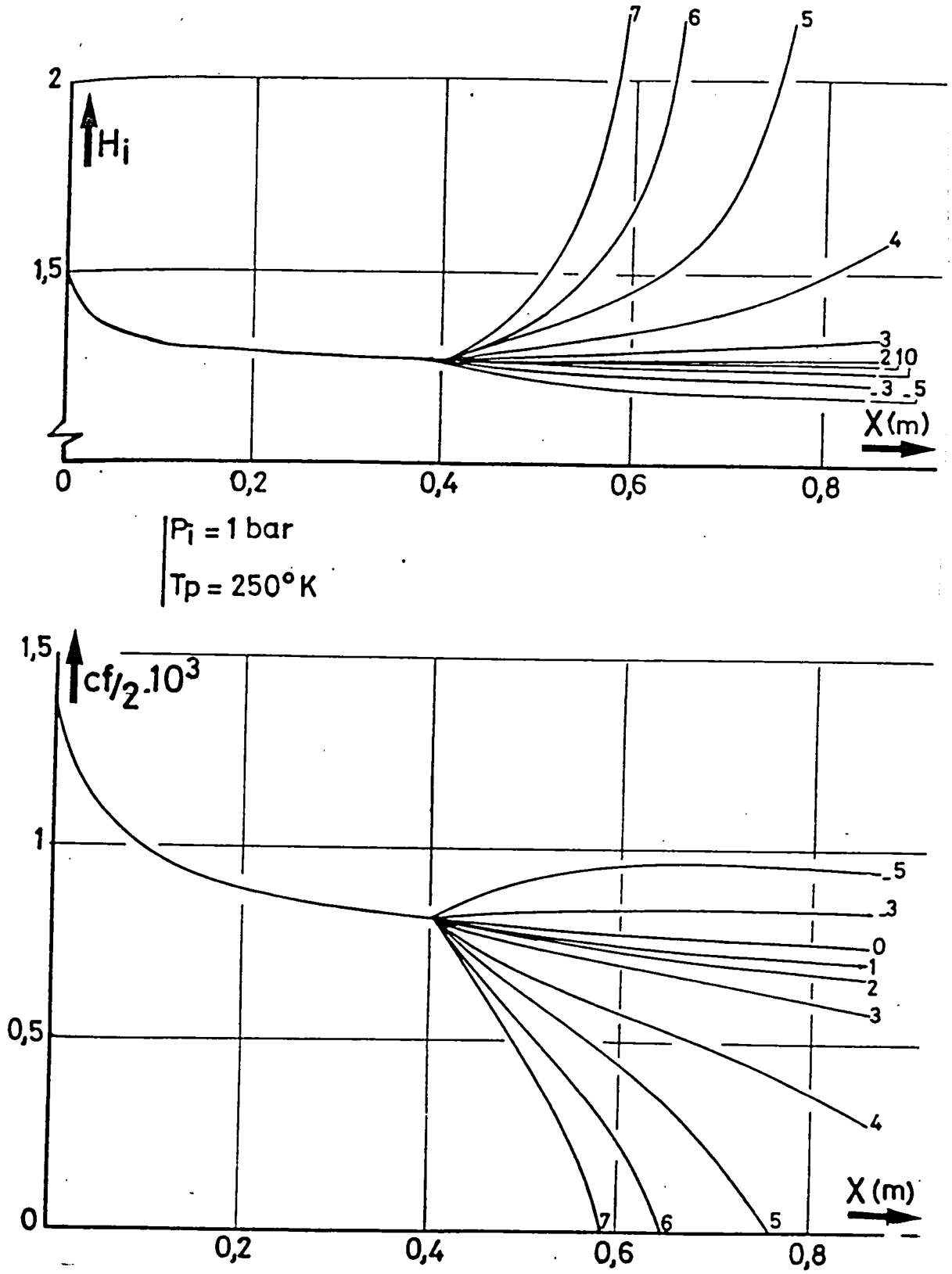

Figure 25 - Hi and Cf = f(x), variable dp/dx.

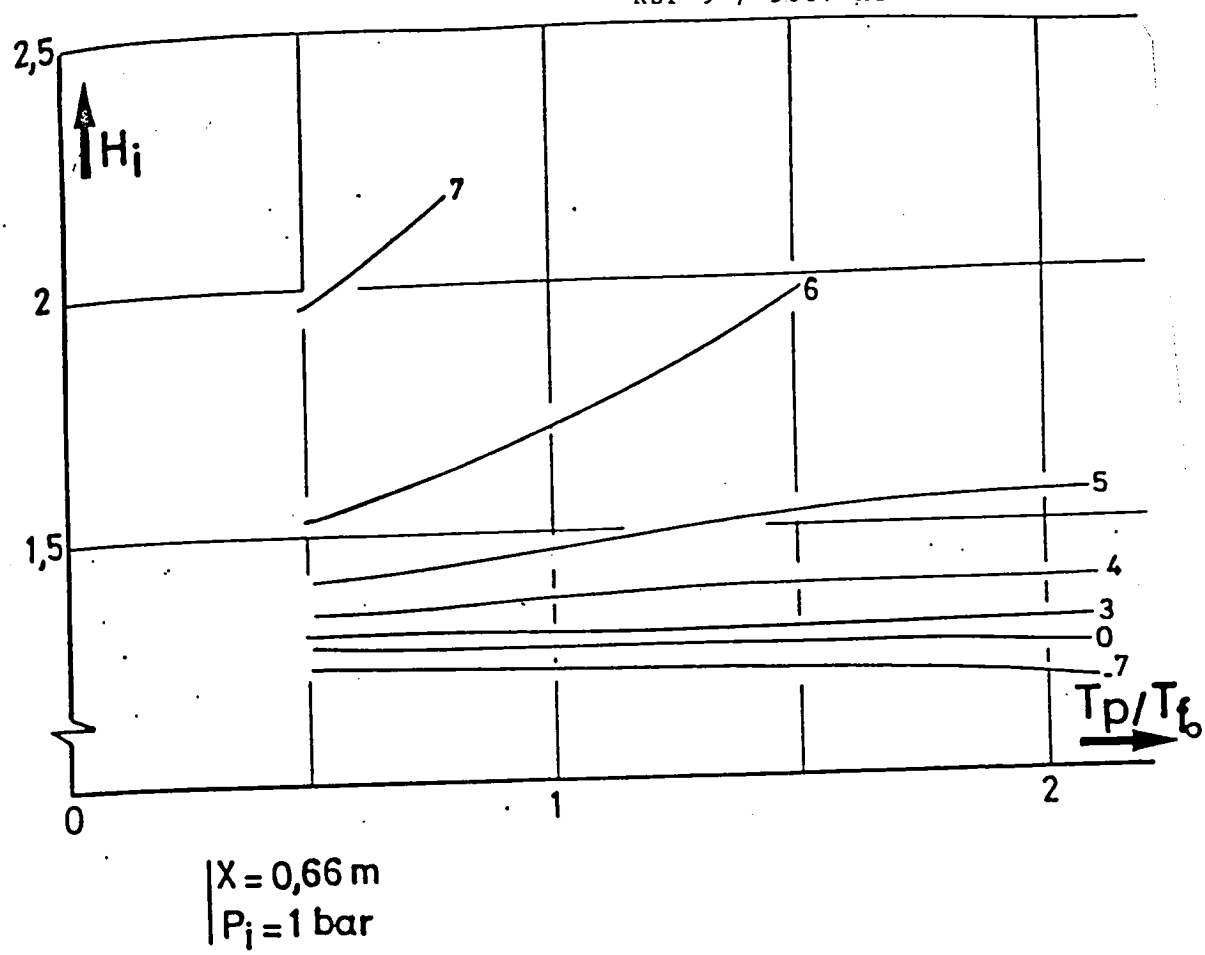

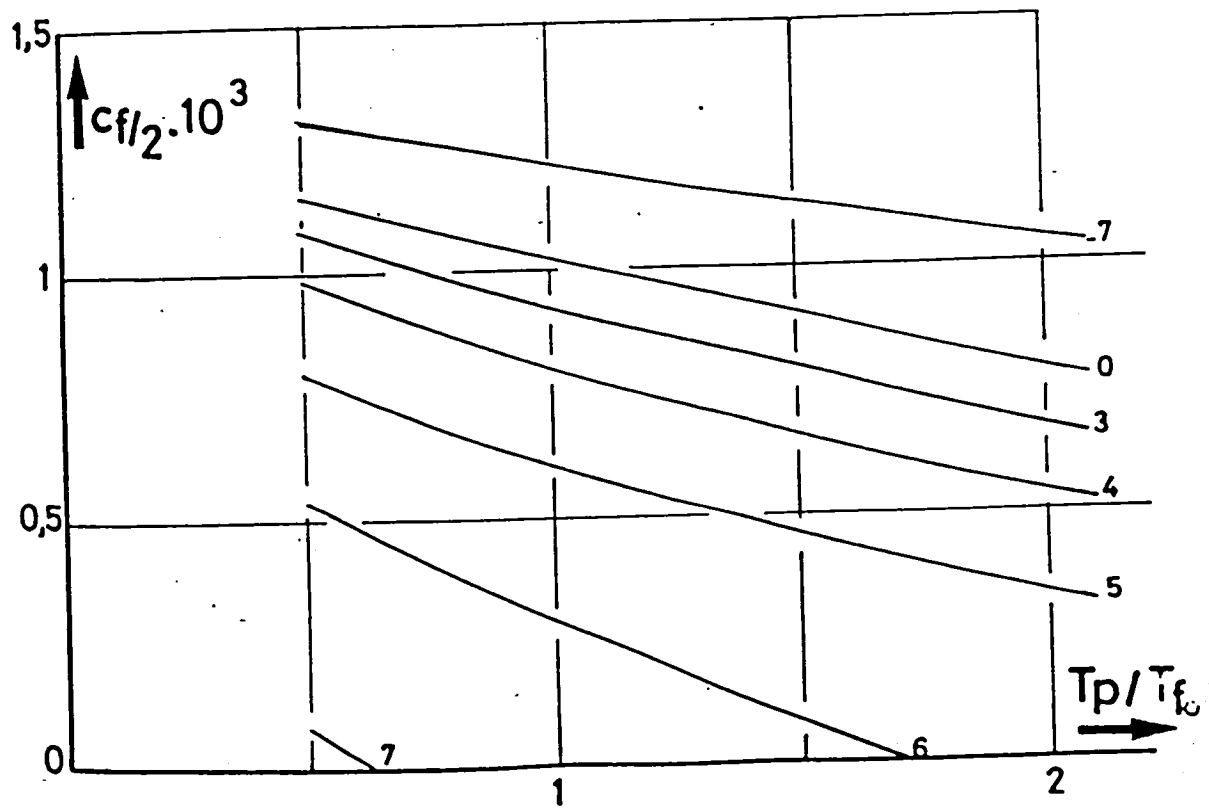

Figure 27 - Hi and Cf - f (Tp/Tfo), varible dp/dx.

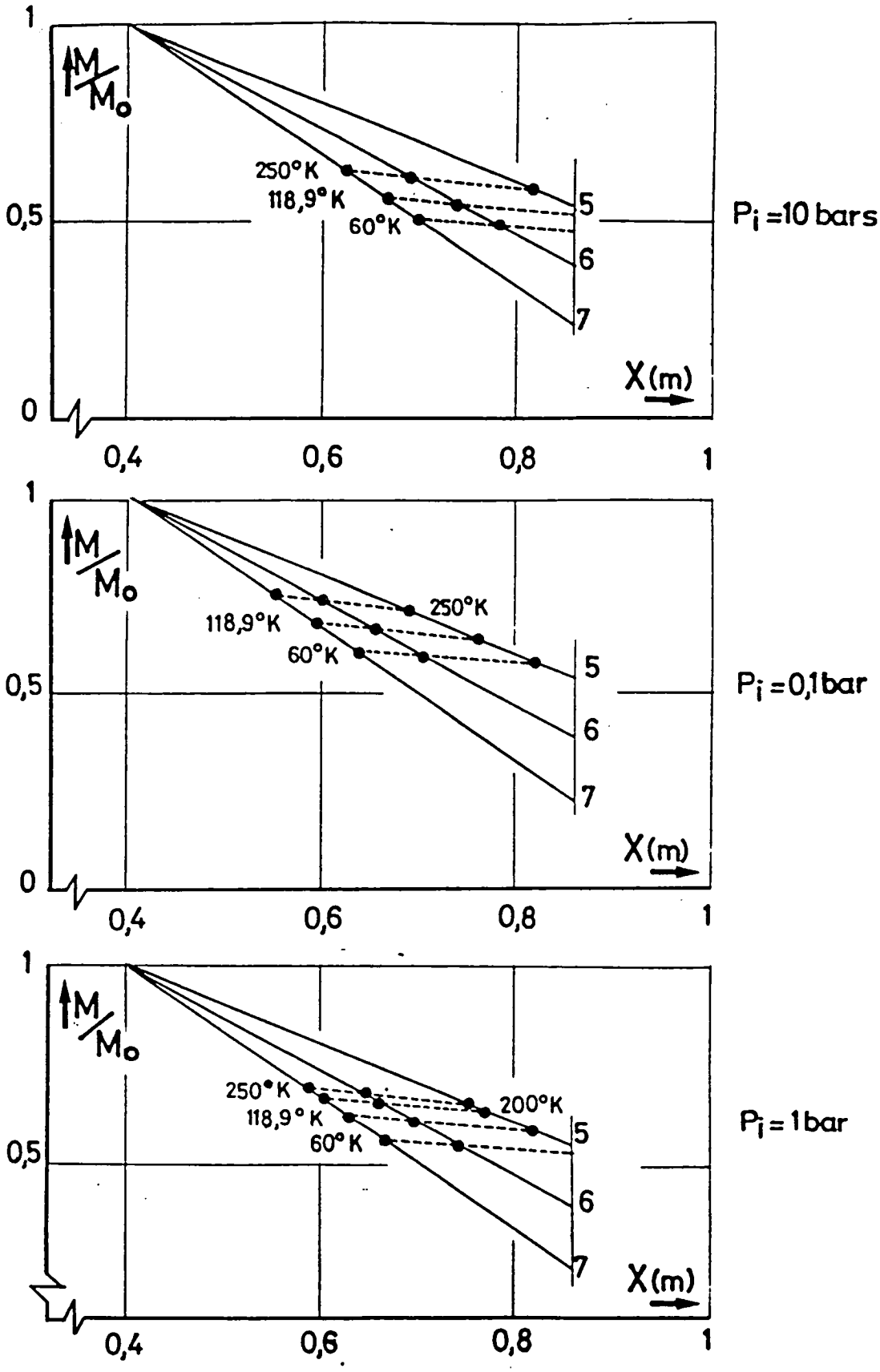

Figure 28 - M/Mo = f(x)